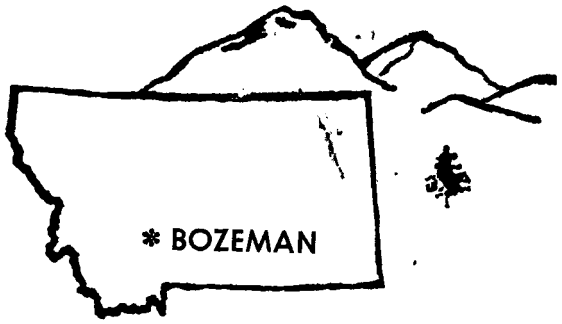

FM DEMODULATOR THRESHOLD REDUCTION

FINAL REPORT
John Duncan,
Project Engineer

Proposal No. EL 63-9
ERL No. 8-0009-623
Contract No. NAS5-3616

Prepared for

National Aeronautics and Space Administration
Goddard Space Flight Center
Glenn Dale Road
Greenbelt, Maryland

Prepared by

Electronics Research Laboratory
Endowment and Research Foundation
Montana State College
Bozeman, Montana

September, 1964

electronics research laboratory

ENDOWMENT AND RESEARCH FOUNDATION AT
MONTANA STATE COLLEGE, BOZEMAN, MONT.

FINAL REPORT

FM DEMODULATOR THRESHOLD REDUCTION

Proposal No. EL 63-9
ERL No. 8-0009-623
Contract No. NAS5-3616

Prepared for

National Aeronautics and Space Administration
Goddard Space Flight Center
Glenn Dale Road
Greenbelt, Maryland

Prepared by

John Duncan, Project Engineer
Electronics Research Laboratory
Endowment and Research Foundation
Montana State College
Bozeman, Montana

September, 1964

19880

ABSTRACT

19880

The results of an investigation of the threshold phenomenon in FM demodulators and techniques for reducing this threshold are described in this paper.

In the initial phase of the investigation, the multitude of literature on this subject was reviewed. A complete list of the pertinent literature is included in the bibliography. A thorough mathematical analysis is presented of the stochastic processes involved in the demodulation of a signal in the presence of band-limited white noise. This analysis results in the derivation of an expression for the signal-to-noise ratio transfer characteristic of a conventional FM demodulator. From this expression, it is obvious that the FM threshold is a function only of the demodulator input signal-to-noise ratio and is independent of the modulation conditions. It is concluded from this that to reduce the threshold, it is necessary to use a form of predetection filtering which can reduce the signal-to-noise ratio at the frequency discriminator input.

Two controversial threshold reduction techniques, the Phase-Locked-Loop (PLL) and the Frequency-Compressive-Feedback-Loop (FCFL) demodulators are discussed and the theory of their operation outlined. A third technique, the Frequency-Tracked-Filter is proposed and a limited investigation of its feasibility presented.

The threshold reduction capabilities of the FCFL demodulator are evaluated from an experimental model. The results of this experimental evaluation lead to the conclusion that, while the idealized FCFL demodulator appears to offer excellent threshold reduction possibilities, several physical limitations severely restrict its capabilities. These restricting factors include a relatively low upper limit on the amount of feedback that may be applied and still maintain a stable system, and the expansion of the noise bandwidth inside the loop which is typical of all negative feedback systems. The PLL and Frequency-Tracked-Filter demodulators appear to have a number of practical advantages over the FCFL demodulator. They are not as susceptible to loop delays and their control loops are not in the signal path.

Author

ACKNOWLEDGMENTS

Most of the mathematical analysis in this paper were stimulated by the excellent literature produced by Dr. E. J. Baghdady. While in all cases, the final results are in full agreement with those of Dr. Baghdady, it was felt necessary to go through their derivations independently because of the difficulty encountered in attempting to justify them as they appeared in the literature.

I wish to acknowledge the very able and indispensible assistance of Mr. Lee Cannon in every phase of this program. Thanks are also extended to Mr. Michael Berkoff for his contributions in the statistical analysis and Mr. Hartvig Melbye for his help in the construction of the experimental models.

TABLE OF CONTENTS

LIST OF ILLUSTRATIONS

1.0 INTRODUCTION

1.1 History and Background

With the advent of space probes came an increased need for light weight, low power, long range telemetry systems. Exponentional modulation schemes, such as large index FM and PM, have some features which place them high on the list of candidates. Although they require rather complex systems, they are, in general, very efficient in terms of power. At the expense of added RF bandwidth, these techniques can yield a considerable increase in baseband signal-to-noise ratio at the receiver output over that obtainable from AM, SSB, and similar schemes using the same transmitter power. This increased baseband signal-to-noise ratio can be exchanged for increased range or a lower power and lighter weight transmitter which would thus reduce power supply requirements.

The baseband signal-to-noise ratio improvement is obtained at the demodulator. That is, the baseband signal-to-noise power ratio, SNR_{bb}, is actually higher than the IF signal-to-noise power ratio, SNR_{IF}. If SNR_{bb} and SNR_{IF} are expressed in decibels, SNR_{bb} varies linearly with SNR_{IF} for large SNR_{IF}. As SNR_{IF} is decreased, however, a point is encountered at which the linear relationship ceases to hold and SNR_{bb} begins to decrease much more rapidly than SNR_{IF}. If the baseband signal is an audio signal, this point, called the threshold, is characterized by very sharp cracking sounds, sometimes called clicks, in the output. As SNR_{IF} is decreased further below the threshold, the clicks diminish and the output becomes the much more gentle white noise. The definition of exactly where the threshold occurs varies drastically from author to author. Some define it as the point where some particular number of clicks per second are heard and others as some particular deviation from linearity. For convenience, it will be defined here as the point where the deviation from linearity is ten percent.

In many instances, the minimum acceptable SNR_{bb} is less than that at which the threshold occurs. Under these conditions, a demodulation technique which exhibits a lower threshold than a conventional FM demodulator would permit useful operation at a lower SNR_{IF}.

Two of the most successful techniques known to date for the reduction of the threshold are the phase-locked loop (PLL) and the frequency compressive feedback loop (FCFL).

The concept of a phase locked loop is not new and has been applied to several different systems problems. As applied to FM demodulation, phase locked loops have been analyzed and tested fairly extensively, but much remains to be done both analytically and experimentally. Many authors disagree on several points in the analysis. Experimental models have thresholds much higher than predicted mathematically.

The frequency compressive feedback loop was first introduced in companion papers by Chaffee [5] and Carson [4] in July, 1939. There has since been several papers written on the FCFL and a few receivers built using this concept, including one for Project Echo. As with the PLL, much disagreement still remains over the theory of the FCFL and thus, much work, both analytic and experimental, remains to be done.

1.2 Contract Objectives

The object of this program is to carefully investigate the threshold phenomenon in FM demodulators. Then, through a thorough examination of the region immediately above and below the threshold point, to report on the feasibility of producing a practical demodulator whose threshold point is lower than the presently known threshold. Also, if it is feasible, to design and build a "breadboard" model of such a demodulator which will exhibit the desired threshold improvement.

1.3 Work Summary

The project was started with an extensive literature search on FM demodulation techniques with emphasis on threshold reduction. The more pertinent articles were then carefully evaluated (second monthly report).

In addition the the facts pointed out in Section 1.1, the following became evident from the literature search:

1) Those authors who have compared PLL and FCFL indicate that PLL is better for low index systems and FCFL is better for high index systems.

2) The mathematical analysis of FM demodulators at and below the threshold region is extremely difficult and frequently claimed to be unsolved.

3) Considerable disagreement exists between authors in the SNR_{bb} vs. SNR_{IF} and the location of the threshold of not only PLL and FCFL but also conventional FM demodulators in the region above the threshold.

4) Very few experimental tests have been published concerning FCFL demodulators.

Since the FCFL demodulator requires a conventional FM detector within its loop, it is necessary to have a coherent analysis of the conventional FM demodulator before the FCFL demodulator can be analyzed. Since no suitable analysis of the conventional FM demodulator could be found in the literature, the project's next task, a lengthy and unexpected one, was to develop such an analysis. The results of this analysis are presented in Section 2.1.

In the early phases of the project, N.A.S.A indicated that they were primarily interested in high modulation index systems. Since the existing literature indicated that FCFL demodulators were superior to PLL demodulators under these conditions, it was decided to center the analysis about the FCFL demodulator. This analysis is presented in Section 2.2.

Section 2.3 gives a very brief description of PLL demodulators.

A third technique, that of a tracking filter between the IF output and the demodulator input, was proposed. This technique, described in Section 2.4, is probably not new. However, until recently, with the introduction of voltage variable capacitors and current variable inductors, was not feasible because no means existed for tuning the filter even at a rate near that of the frequency variation of an FM signal carrying audio information. A very brief analysis was conducted and two very crude breadboard models, one tube and one solid state, were constructed. Although

initial tests indicated that this approach to threshold reduction shows promise, lack of time and finances made it essential to defer further analysis and experimentation.

Since very little experimental research had been done with FCFL demodulators, it was deemed useful to design and construct a breadboard model of such a demodulator. The experimental results obtained from this model are discussed in Section 3.

2.0 ANALYSIS OF DEMODULATION TECHNIQUES

2.1 Conventional FM Demodulator

2.1.1 Introduction to the Conventional FM Demodulator

Conventional FM demodulators include such types as the ratio detector, the Foster-Seely discriminator, balanced discriminator, and the gated-beam discriminator. They consist of an amplitude insensitive device whose output is proportional to the time derivative of the phase of the IF signal. This section gives a brief and hopefully coherent analysis of the demodulation process. Symbols for the variables and constants have been selected so as to remain as consistent as possible with the current literature.

It will be assumed that the reader is familiar with the basics of FM modulation and communication theory and has some understanding of the fundamentals of statistics and integral calculus.

2.1.2 Derivations on Conventional FM Demodulators

Let $u(t)$ be any baseband information function of bandwidth BW_{bb}. A noise-free FM signal carrying this information signal can be represented mathematically as:

$$\begin{aligned} e(t) &= E \cos\left[\omega_c t + \Delta\omega_c \int u(t)\, dt \right] \\ &= E \cos\left[\omega_c t + \psi(t) \right] \end{aligned} \tag{1}$$

where:

$\Delta\omega_c$ is the deviation in radians.

The information is thus proportional to the time varying portion of the time derivative of the phase of $e(t)$. Let BW_{IF} be the IF bandwidth required to pass, relatively undistorted, the signal, $e(t)$.

If white noise is assumed to be present at the receiver input, its bandwidth will be limited to BW_{IF} by IF filtering. Since, generally, $BW_{IF} \ll \omega_c$, the IF noise will be narrow-band gaussian and thus can be represented by the narrow-band random process described by:

$$n(t) = V(t) \cos \left[\omega_c t + \phi (t) \right] \tag{2}$$

where $V(t)$ is Rayleigh distributed and $\phi(t)$ is uniformly distributed from 0 to 2π. The statistical properties of $n(t)$ are discussed in Appendix I.

In most of the derivations to follow, the argument, t), will be dropped. Keep in mind that E is not a function of time but is an amplitude constant.

The signal at the IF output or the demodulator input will consist of the desired FM signal and an additive noise.

$$e_{IF} = e(t) + n(t) . \tag{3}$$

In Appendix II, it is shown that this may be expressed as:

$$e_{IF} = \left[(E + X_c)^2 + X_q^2 \right]^{1/2} \cos \left[\omega_{IF} t + \psi - \tan^{-1} \frac{X_q}{(E + X_c)} \right] \tag{4}$$

and the demodulator output as:

$$e_o = \dot{\psi} + \frac{\frac{\dot{X}_q}{E} \left(1 + \frac{X_c}{E}\right) - \frac{X_q \dot{X}_c}{E^2}}{\left(1 + \frac{X_c}{E}\right)^2 + \left(\frac{X_q}{E}\right)^2} \tag{5}$$

where

$$X_c = V \cos(\psi - \phi)$$
$$X_q = V \sin(\psi - \phi). \tag{6}$$

The first term of Eq. (5) is the desired baseband information signal and the second term is the baseband noise.

In Appendix III, the mean square value of the baseband noise term is shown to be:

$$\overline{n^2} = \frac{\overline{\dot{X}_q^2}}{E^2}\left(1 + \frac{2\sigma^2}{E^2} + \frac{8\sigma^4}{E^4} + \dots\right) \tag{7}$$

where σ^2 is the variance of the noise and is equal to the input noise power normalized to one ohm.

The peak input signal, E, is equal to $\sqrt{2}\, E_{rms}$. Thus, E^2 is equal to twice the input signal power normalize to one ohm.

Hence:

$$\frac{\sigma^2}{E^2} = \frac{1}{2\ SNR_{IF}} \tag{8}$$

and:

$$\overline{n^2} = \frac{\overline{\dot{X}_q^2}}{E^2}\left(1 + \frac{1}{SNR_{IF}} + \frac{2}{(SNR_{IF})^2} + \dots\right) \tag{9}$$

It is shown in Appendix IV that:

$$\overline{\dot{X}_q^2} \approx \sigma^2 \frac{8\pi^2 (BW_{bb})^3}{3(BW_{IF})}. \tag{10}$$

Substituting Eq. (10) into Eq. (9) gives:

$$\overline{n^2} \approx \frac{8\pi^2 (BW_{bb})^3 \sigma^2}{3(BW_{IF})E^2} \left(1 + \frac{1}{SNR_{IF}} + \frac{2}{(SNR_{IF})^2}\right). \tag{11}$$

Assume:

$$\psi = M_f \sin \omega_m t \tag{12}$$

where:

$$M_f = \frac{\Delta \omega_c}{\omega_m} \quad \text{is the modulation index.} \tag{13}$$

Then:

$$\dot{\psi} = \Delta \omega_c \cos \omega_m t \tag{14}$$

and:

$$\overline{\dot{\psi}^2} = \frac{\omega_m}{2\pi} \int_0^{\frac{2\pi}{\omega_m}} \Delta \omega_c^2 \cos^2 \omega_m t dt = \frac{\Delta \omega_c^2}{2}. \tag{15}$$

Substituting Eqs. 8, 11, 13, 15, and $4\pi^2 (BW_{bb})^2 = \omega_m^2$ into:

$$SNR_{bb} = \frac{\overline{\dot{\psi}^2}}{\overline{n^2}}$$

and simplifying gives the baseband signal-to-noise ratio as:

$$SNR_{bb} = \frac{3}{2} M_f^2 \, SNR_{IF} \, \frac{BW_{IF}}{BW_{bb}} \left[\frac{1}{\left(1 + \frac{1}{SNR_{IF}} + \frac{2}{(SNR_{IF})^2} \cdots\right)}\right]. \tag{16}$$

From this expression, it is apparent that the SNR_{bb} is a linear function of SNR_{IF} until the bracketed term becomes significant. The threshold will be defined as that point where the contributions from the bracketed term causes SNR_{bb} to deviate by 10% from the straight line relation. We may assume this occurs approximately when $\frac{1}{SNR_{IF}} = \frac{1}{10}$. The threshold can then be said to occur at $SNR_{IF} = 10$ (or 10 db).

For very high modulation indexes ($M_f > 5$):

$$BW_{IF} = 2(\Delta \omega_c/2\pi)$$

$$BW_{bb} = (\omega_m/2\pi)$$

and thus:

$$SNR_{bb} \approx 3 M_f^3 SNR_{IF} \left(\frac{1}{1 + \frac{1}{SNR_{IF}} + \frac{2}{SNR_{IF}^2} + \ldots} \right). \quad (17)$$

For very low modulation indexes ($M_f < .6$):

$$BW_{IF} = 2(\omega_m/2\pi)$$

$$BW_{bb} = (\omega_m/2\pi)$$

and thus:

$$SNR_{bb} \approx 3 M_f^2 SNR_{IF} \left(\frac{1}{1 + \frac{1}{SNR_{IF}} + \frac{2}{SNR_{IF}^2} + \ldots} \right). \quad (18)$$

2.1.3 Discussion of Conventional FM Demodulators

The signal-to-noise transfer characteristics of a conventional FM demodulator are given by Eqs. (17) and (18) and are plotted in Figure 1.

Note that the threshold occurs at 10 db regardless of the modulation index. At first glance, this would seem to imply that SNR_{bb} could be increased indefinitely merely by increasing M_f. However, if M_f is increased, the IF bandwidth must be increased to accomodate the signal. This will increase the noise bandwidth and thus decrease SNR_{IF} for the same signal power. An excessive increase in M_f will cause SNR_{IF} to fall below the threshold.

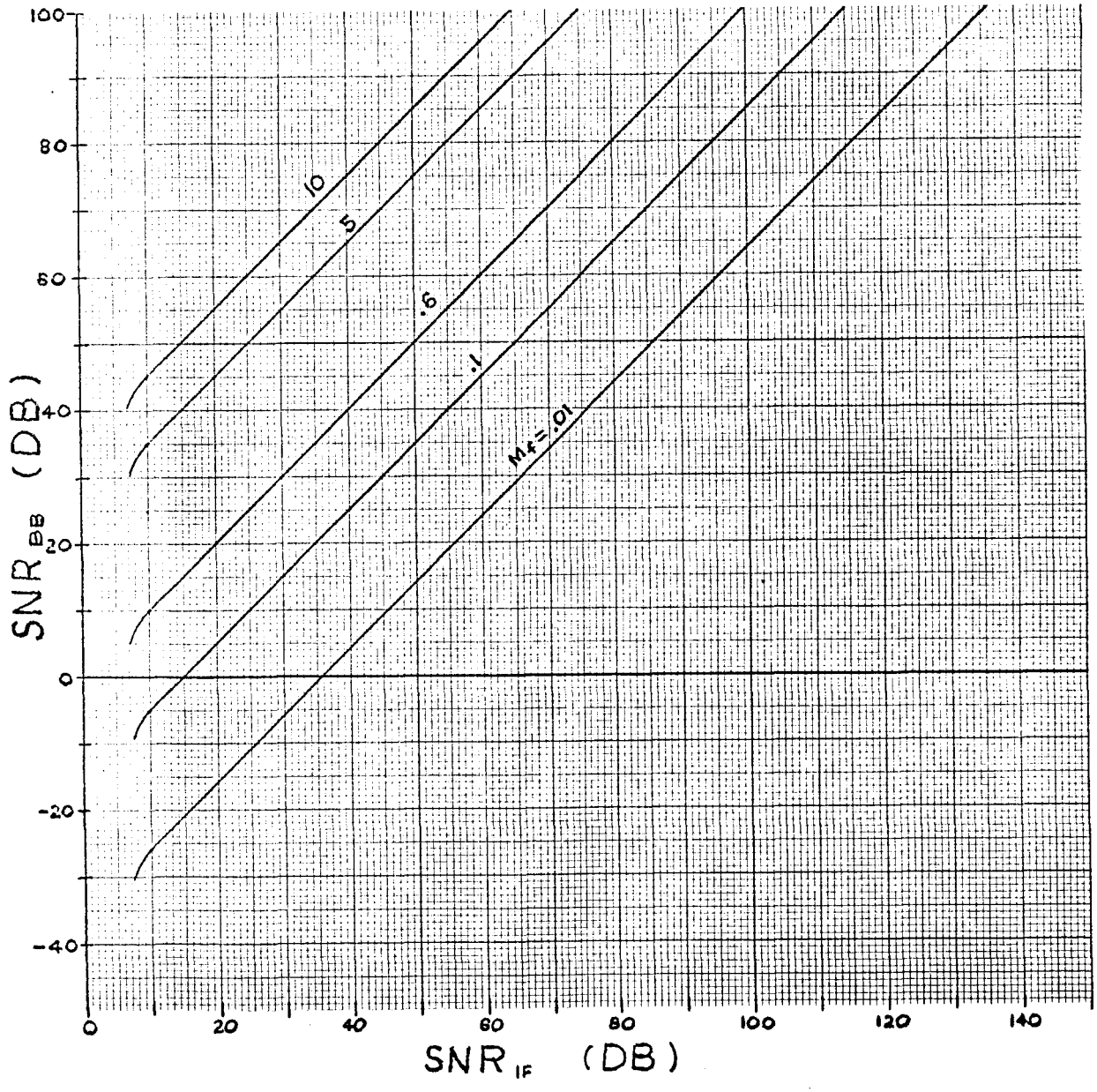

Figure 1. Signal-to-Noise Transfer Characteristic of a Conventional FM Demodulator.

For $M_f = 1/\sqrt{3} \approx .6$ and $SNR_{IF} > 10$, Eq. (18) gives $SNR_{bb} = SNR_{IF}$. This point (i.e., $M_f = 1/\sqrt{3}$) is defined as the line between narrowband FM(NBFM) and wideband FM(WBFM).

2.1.4 Approaches to the Improvement of FM Demodulation

In the case of linear modulation techniques such as AM and SSB, where a linear relationship exists between the high and low frequencies of the message or baseband signal and the RF or IF signal, if adequate RF or IF filtering is provided, additional baseband filtering after demodulation will not improve the SNR_{bb}. This is not the case, however, for a non-linear or bandwidth expanding modulation technique such as FM. In this case, the RF signal bandwidth may be many times that of the baseband and no such linear correspondence exists between the frequency components of the baseband and the RF signal. For WBFM, if the IF bandwidth is made as narrow as possible while still passing all those RF components necessary to faithfully reproduce the baseband signal, there will still exist noise components on the IF signal which yield frequency components at baseband which can extend well above the highest desired baseband frequency. No amount of fixed predetection filtering can remove these noise components. After detection, the noise component above the highest information signal frequency can be removed by good lowpass filtering and thus, the improvement of SNR_{bb} over SNR_{IF}. This belated filtering makes it necessary to operate the demodulator at an SNR_{IF} much greater than SNR_{bb}. Above the threshold, nothing is lost by this process since SNR_{IF} and SNR_{bb} are linearly related.

It was proven in Section 2.1.2 that the threshold occurred at a specific SNR_{IF} (SNR_{IF} = 10 db). Obviously, if some technique could be devised for removing from the IF signal, that noise which yields baseband frequencies greater than the information signal, prior to detection, SNR_{IF} could be substantially increased and the threshold thus reduced.

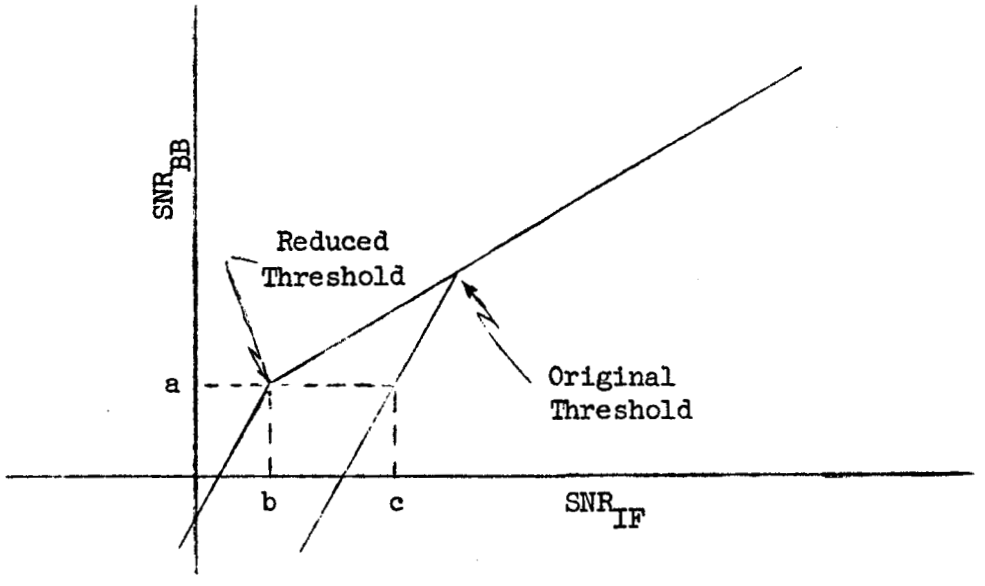

Figure 2. Threshold Reduction Due to Predection Filtering

Figure 2 demonstrates the advantage of this predetection filtering over postdetection filtering. Let point "a" represent the minimum acceptable SNR_{bb}. Predetection filtering then permits operation at an SNR_{IF} as low as point "b." On the other hand, postdetection filtering may not be used with an SNR_{IF} any lower than point "c."

As pointed out above, the predetection filtering cannot be done with a standard bandpass filter since the high frequencies in the baseband do not necessarily correspond to the frequencies near either of the band edges of the IF signal as in AM and SSB.

An FM signal can be visualized as a single spectral component moving about within a bandwidth of $2 \Delta \omega_c$. Since the baseband signal is the time derivative of this frequency change, the rate of change of frequency is equal to the baseband frequency. The maximum rate of change of frequency desired in the IF signal is thus given by the maximum frequency of the information signal. However, when random noise has been added to the RF signal, variations of higher frequency will be present. These rapid variations yield the high frequency components in the baseband signal.

Three techniques for the reduction of these high frequency variations will be presented here. These are the frequency compressive feedback loop, the phase locked loop, and the tracking filter.

2.2 Frequency Compressive Feedback Loop (FCFL)

2.2.1 Introduction to the FCFL Demodulator

The frequency compressive feedback loop demodulator is the most sophisticated of the three systems to be discussed here. This approach relies upon feedback from the processed FM signal to compress a WBFM signal to a NBFM signal ($M_f \approx 1/\sqrt{3}$). Figure 3 shows a block diagram of an FCFL demodulator.

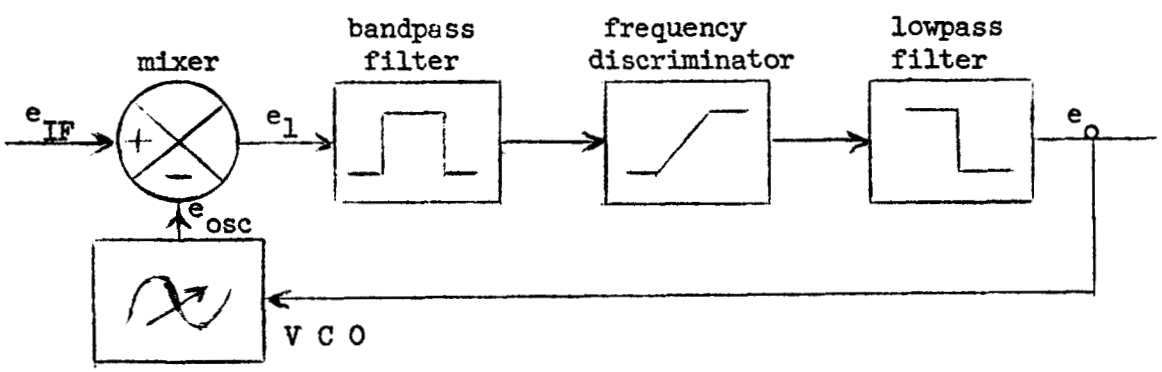

Figure 3. Block Diagram of an FCFL Demodulator

The VCO (voltage controlled oscillator) is adjusted so that it will be modulated by the baseband signal at a modulation index just slightly less than the modulation index of the IF signal. When the output of the VCO is mixed with the IF signal and the difference frequency retained, the input to the detector will be an FM signal with a modulation index equal to the difference of the modulation indexes of the IF signal and the VCO output. This signal is then detected to give the baseband signal.

Perhaps the simplest nonrigorous qualitative explanation of the operation of the idealized FCFL demodulator is in terms of the frequency spectrum. Assume the IF signal has been modulated by the highest frequency of information signal. Since this gives a WBFM signal, its spectral density function will be similar to Figure 4a. As pointed out in section 2.1.4, the high frequencies at baseband corresponded to the more rapid frequency changes in the IF signal. Conversely, the low frequencies at baseband correspond to the slower frequency changes in the IF signal. Since the IF bandwidth is limited to BW_{IF}, the baseband noise spectral components which lie above the highest information signal frequency must have corresponding IF signal components as illustrated in Figure 4b, of lower modulation index than the information signal, in order to have been passed by the IF filter. The low frequency spectral noise components may correspond to the spectral density functions given by Figures 4c or 4d.

Assume that a baseband signal is available which contains only the information signal and noise of frequencies less than or equal to the highest frequency in the information signal. If this signal is used to modulate the VCO, the VCO output will contain spectral components similar to those given in Figures 4e through 4h.

The modulation index of this signal has been chosen to be slightly less than that of the IF signal. If these two signals are then mixed and the difference frequencies retained, the mixer output will contain the spectral components shown in Figures 4i through 4l.

Note that the spectral components corresponding to the information signal and to the low frequency baseband noise have been compressed to a bandwidth of twice the highest frequency of the information signal, $2 f_m$. However, the components corresponding to the high baseband frequencies were not compressed. The mixer output can now be limited to a bandwidth of $2 f_m$ without deteriorating the information signal. This gives a detector input containing the components shown in Figures 4m through 4p. The detector output will thus be the required baseband signal containing no noise components higher than f_m.

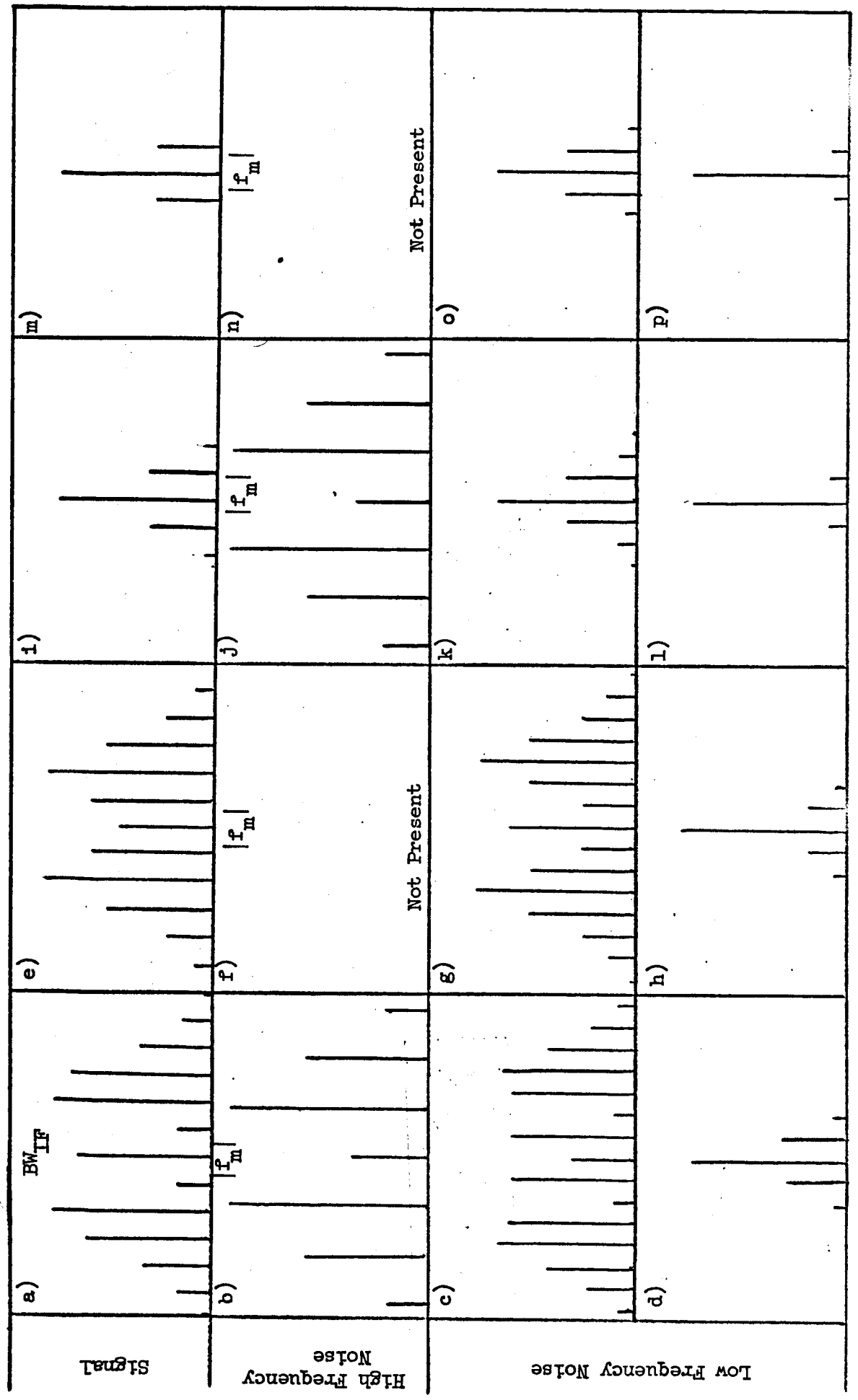

Figure 4. Spectral Components in an FCFL Demodulator

The FCFL demodulator is thus a predetection filtering technique and, as pointed out in section 2.1.4, should provide a reduction in the FM threshold.

2.2.2 Derivations on the FCFL Demodulator

The reduction in modulation index initiated by the FCFL demodulator can readily be shown by the following elementary analysis.

From Eq. (4):

$$e_{IF} = \left[(E + X_c(t))^2 + X_q^2(t) \right]^{1/2} \cos \left[\omega_{IF} t + M\phi(t) - \tan^{-1} \frac{X_q(t)}{E + X_c(t)} \right] \tag{19}$$

where:

$$M\phi(t) = \psi(t) .$$

Assume:

$$e_{osc} = E_{osc} \cos \left[\omega_o t + K_f M\phi(t) - \alpha(t) + \theta \right] . \tag{20}$$

If the difference frequency only is retained at the mixer output:

$$e_1 = E_{osc} \left[(E + X_c(t))^2 + X_q^2(t) \right]^{1/2} \cos \left[(\omega_{IF} - \omega_o)t + (1 - K_f)M\phi(t) \right.$$

$$\left. + \alpha(t) - \tan^{-1} \frac{X_q(t)}{E + X_c(t)} - \theta \right] . \tag{21}$$

The detector output is thus:

$$e_o = K_d \left[(1 - K_f) M\phi'(t) + \alpha'(t) - \frac{d}{dt} \left[\tan^{-1} \frac{X_q(t)}{E + X_c(t)} \right] \right] \tag{22}$$

where K_d volts per cycle is the sensitivity of the detector.

If this signal is used to modulate a VCO of sensitivity K_v cycles per volt, the VCO output is given by:

(23)

$$e_{osc} = E_{osc} \cos \left[\omega_o t + K_v K_d (1 - K_f) M\phi(t) + \alpha(t) - \tan^{-1} \frac{X_q(t)}{E + X_c(t)} + \theta \right].$$

Equating Eqs. (20) and (23) gives:

$$K_f M\phi(t) = K_v K_d (1 - K_f) M\phi(t) \tag{24}$$

$$\alpha(t) = K_v K_d \left[\alpha(t) - \tan^{-1} \frac{X_q(t)}{E + X_c(t)} \right]. \tag{25}$$

This gives:

$$K_f = \frac{K_d K_v}{1 + K_d K_v} \tag{26}$$

and:

$$\alpha(t) = \left[\frac{K_d K_v}{1 + K_d K_v} \right] \tan^{-1} \frac{X_q(t)}{E + X_c(t)}. \tag{27}$$

Thus:

$$e_1 = E_{osc} \left[(E + X_c(t))^2 + X_q^2(t) \right]^{1/2} \cos \left[(\omega_{IF} - \omega_o)t + \left(\frac{M}{1 + K_d K_v}\right) \phi(t) \right.$$

$$\left. - \left(\frac{1}{1 + K_d K_v}\right) \tan^{-1} \frac{X_q(t)}{E + X_c(t)} - \theta \right] \tag{28}$$

$$e_o = \frac{K_d M}{1 + K_d K_v} \phi'(t) - \frac{K_d}{1 + K_d K_v} \frac{d}{dt} \left[\tan^{-1} \frac{X_q(t)}{E + X_c(t)} \right]. \qquad (29)$$

The reduced modulation index, $M/(1 + K_d K_v)$, can readily be seen in Eq. (28).

From the qualitative description of the FCFL demodulator presented above, it would seem that the lowpass filter is of no use. The predetection filtering, given by the compression of the deviation and the IF bandpass filtering, would seem to be capable of removing any noise which the lowpass, postdetection, filter could remove. This would be the case if it were not for the bandwidth expansion inherent in any system using negative feedback.

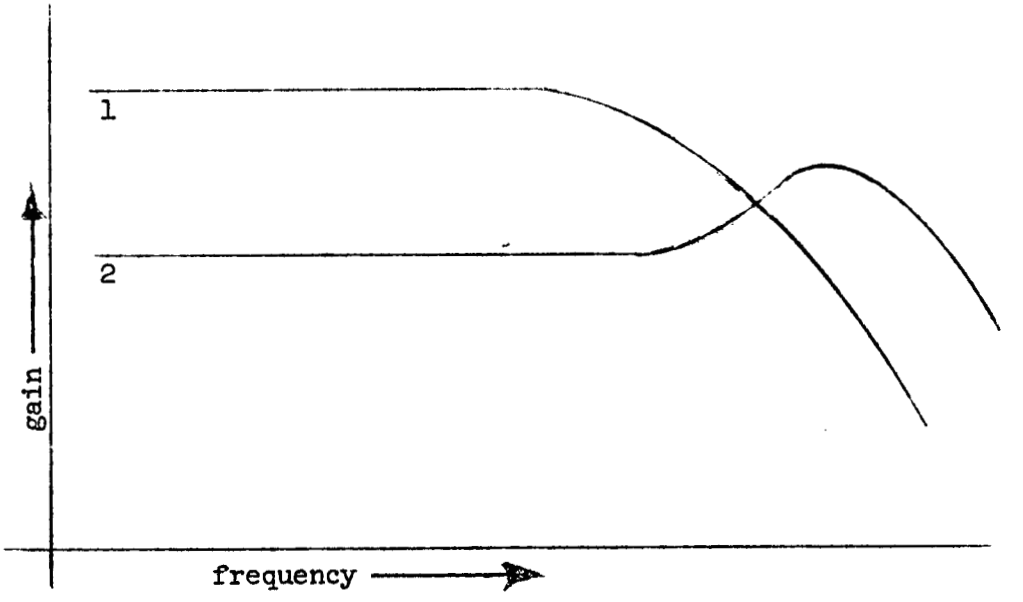

Figure 5. Bandwidth Expansion Caused by Negative Feedback

That is, a system having an open loop bandwidth given by curve 1 in Figure 5 would have a closed bandwidth similar to that given by curve 2. Thus, if the signal at the output of the mixer deviates only as far as the cutoff points of the bandpass filter, the noise bandwidth will be much wider than the signal bandwidth. The low pass filter may be used to alter this noise bandwidth. The effects

of the lowpass filter may be demonstrated quantitatively with the aid of a baseband analog of the FCFL demodulator. Such a model is shown in Figure 6.

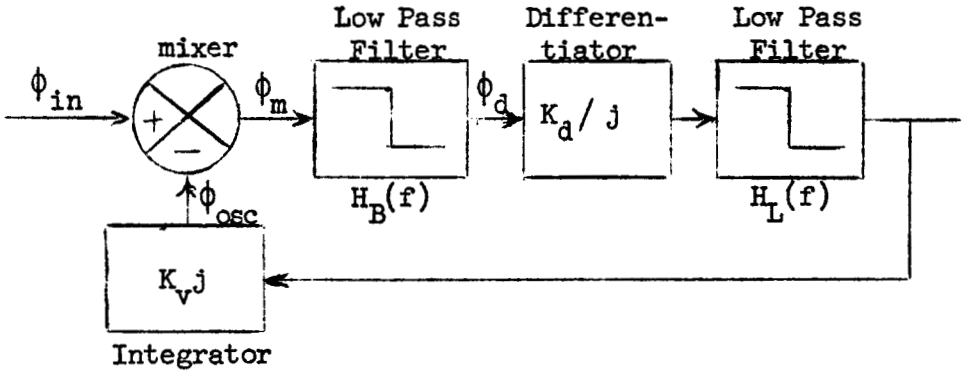

Figure 6. Baseband Analog of an FCFL Demodulator

where:

$$H_B(f) = \frac{H_1}{1 + j\frac{f}{kF_b}} \qquad H_L(f) = \frac{H_2}{1 + j\frac{f}{f_b}} \tag{30}$$

f_b = 3 db frequency of the lowpass filter

$2kf_b$ = 3 db bandwidth of bandpass filter.

Let $A = H_B K_d$ and $\beta = H_L K_v$.

Then:

$$\frac{\phi_m}{\phi_{in}} = \frac{1}{1 + K_d K_v H_B(f) H_L(f)} \tag{31}$$

and:

$$\frac{\phi_{osc}}{\phi_{in}} = \frac{K_d K_v H_B(f) H_L(f)}{1 + K_d K_v H_B(f) H_L(f)} \tag{32}$$

and:

$$\frac{\phi_d}{\phi_{in}} = \frac{H_B(f)}{1 + K_d K_v H_B(f) H_L(f)} \, . \tag{33}$$

The compressed modulation index can again be seen from Eq. (31).

Substituting Eq. (30) into Eqs. (32) and (33) and normalizing to unity at f = 0 for ease of comparison yields:

$$\left(\frac{\phi_{osc}}{\phi_{in}}\right)_{norm} = \frac{1 + A\beta}{\left[(1 + A\beta) - \frac{1}{k}\left(\frac{f}{f_b}\right)^2\right] + j\left(1 + \frac{1}{k}\right)\frac{f}{f_b}} \tag{34}$$

$$\left(\frac{\phi_d}{\phi_{in}}\right)_{norm} = \frac{(1 + A\beta)\left(1 + j\,\frac{f}{f_b}\right)}{\left[(1 + A\beta) - \frac{1}{k}\left(\frac{f}{f_b}\right)^2\right] + j\left(1 + \frac{1}{k}\right)\frac{f}{f_b}} \, . \tag{35}$$

Plots of the magnitudes and phases of these two functions for various values of k and $A\beta$ ($K_d K_v$ when normalized) are given in Appendix V. The noise bandwidth expansion pointed out in Figure 5 can readily be seen in these plots. If the noise spectral density is assumed to be uniformly distributed, the noise power will be proportional to the area under the magnitude squared curve.

This area can be calculated from Eq. (34):

$$\int_{-\infty}^{\infty} \left| \frac{\phi_{osc}}{\phi_{in}} \right|^2 df = \int_{-\infty}^{\infty} \frac{(1 + A\beta)^2 k^2 f_b}{\left(\frac{f}{f_b}\right)^4 + \left[(1 + k)^2 - 2k(1 + A\beta)\right]\left(\frac{f}{f_b}\right)^2 + (1 + A\beta)^2 k^2} d\left(\frac{f}{f_b}\right)$$

$$= \frac{(1 + A\beta)\, k\pi f_b}{1 + k}$$

$$= \frac{(1 + A\beta)\, \pi f_{if}}{2} \left(\frac{1}{1 + 1/2\, C} \right). \qquad (36)$$

and from Eq. (35):

$$\int_{-\infty}^{\infty} \left| \frac{\phi_d}{\phi_{in}} \right|^2 df = \int_{-\infty}^{\infty} \frac{(1 + A\beta)^2 k^2 f_b \left[1 + \left(\frac{f}{f_b}\right)^2 \right]}{\left(\frac{f}{f_b}\right)^4 + \left[(1 + k)^2 - 2k(1 + A\beta)\right]\left(\frac{f}{f_b}\right)^2 + (1 + A\beta)^2 k^2} d\left(\frac{f}{f_b}\right)$$

$$= \frac{(1 + A\beta)\, k\pi f_b \left[1 + k(1 + A\beta) \right]}{1 + k}$$

$$= \frac{(1 + A\beta)\, \pi f_{if}}{2} \left(1 + \frac{A\beta}{1 + 2C} \right) \qquad (37)$$

where:

$f_b = Cf_{if}$

f_{if} = IF filter bandwidth.

Let:

$$F(A\beta, f_{if}) = \frac{(1 + A\beta)\,\pi f_{if}}{2} . \tag{38}$$

Then Eq. (36) gives:

$$N_1 = \int_{-\infty}^{\infty} \left| \frac{\phi_{osc}}{\phi_{in}} \right|^2 df = F(A\beta, f_{if}) \left(\frac{1}{1 + 1/2\,C}\right) \tag{39}$$

and Eq. (37) gives:

$$N_2 = \int_{-\infty}^{\infty} \left| \frac{\phi_{d}}{\phi_{in}} \right|^2 df = F(A\beta, f_{if}) \left(1 + \frac{A\beta}{1 + 2\,C}\right) \tag{40}$$

Figure 7 shows a rough plot of these two functions as C is varied.

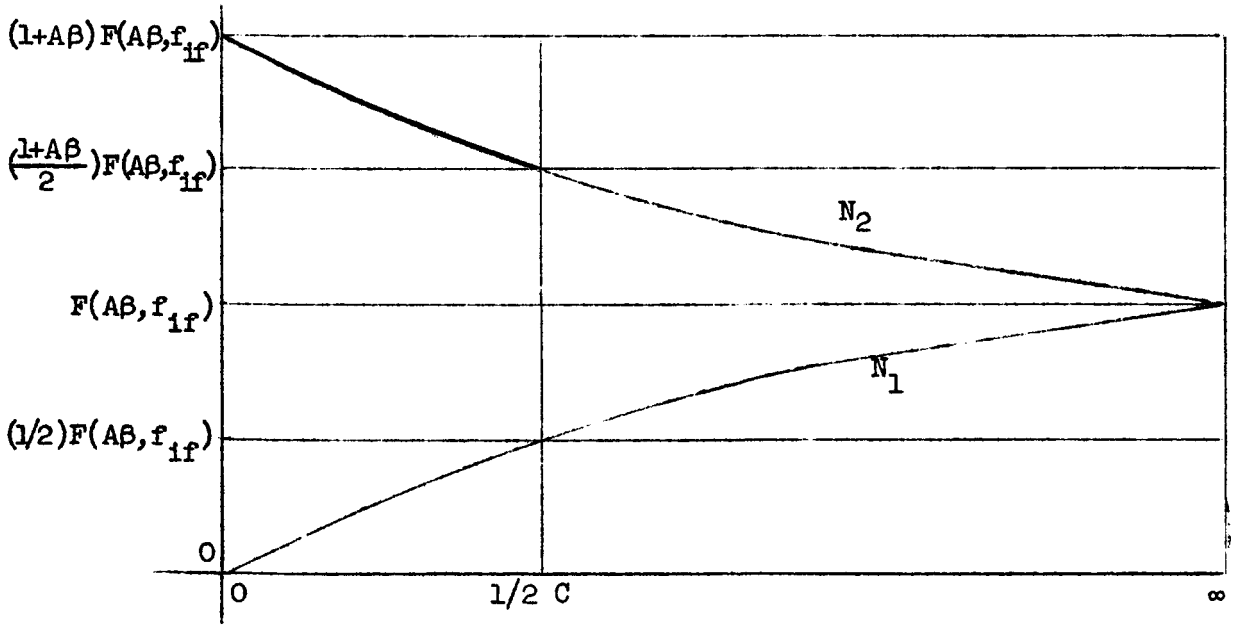

Figure 7. The Effect of the Lowpass Filter Upon the Noise Bandwidth

2.2.3 Discussion of the FCFL Demodulator

C is the ratio of the lowpass filter bandwidth to the bandpass filter bandwidth. Thus, an infinite C corresponds to the removal of the lowpass filter. From Figure 7, it is apparent that the noise bandwidth at the detector input is minimum under this condition. However, the noise bandwidth at the oscillator output is maximum under these conditions. If the noise power at the detector input would remain linearly related to the input IF noise power, this would be the optimum point. This is not the case, however. There are several factors which tend to increase the noise at the output of the VCO. Time delay around the loop can give incoherence with the IF signal at the mixer resulting in new noise components. At low SNR_{IF}, the cophase components of the noise, X_c, which at high SNR_{IF} contribute primarily amplitude variations, appear in the baseband signal and thus phase modulate the VCO giving more noise components. Cross products of noise from the VCO and from the IF input in the mixer add additional components. Distortions, non-linearities, imperfect limiting or amplitude rejection, and other practical problems add still more noise. Phase characteristics require that the filters have only single poles. This leaves a considerable amount of high frequency noise at baseband which should be removed. All of these properties make it desirable to do additional filtering at baseband.

The above discussion tends to indicate the presence of two thresholds. One of these is the previously discussed threshold of the conventional demodulator. The other, called a closed loop threshold, is caused by the various added noise sources mentioned above. This threshold will obviously be minimum when C = 0 (see curve N_1 in Figure 7) since this corresponds to a low pass filter of zero bandwidth and then no noise (or signal) is fed into the VCO. Logically, the lowpass filter bandwidth should be set so that the two thresholds occur at the same SNR_{IF}. The evaluation of the theoretically optimum bandwidth would require the evaluation of a number of covariances, a lengthy and complex procedure.

This, as yet, has not been done. Much additional analysis could be done on the FCFL Demodulator.

2.3 Phase Locked Loop (PLL)

2.3.1 Introduction to the PLL Demodulator

The phase locked loop, probably the most obvious approach to predetection filtering, consists of an oscillator, phase locked to the IF signal. It is designed so that the oscillator frequency cannot be made to vary faster than the highest frequency of the information signal.

Figure 8 shows a block diagram of the phase locked loop.

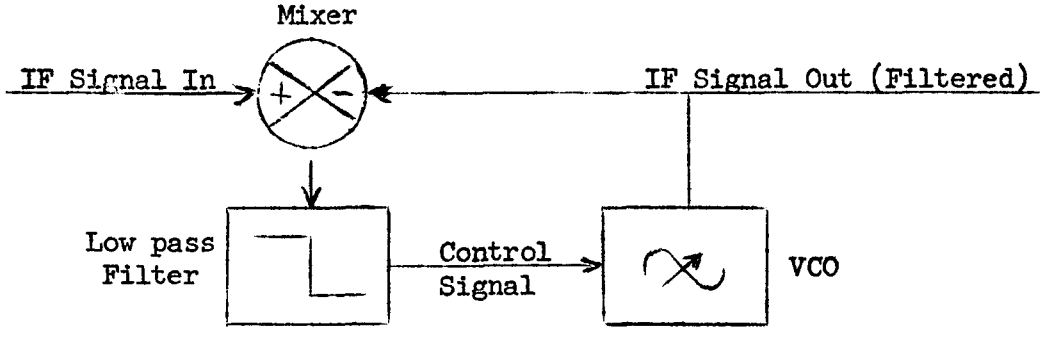

Figure 8. Block Diagram of a PLL Demodulator

2.3.2 Discussion of the PLL Demodulator

The output signal from a phase locked loop is derived from a voltage controlled oscillator with a center frequency equal to the IF carrier frequency. A mixer or phase detector is used to obtain

a voltage proportional to the difference between the VCO frequency and the instantaneous frequency of the IF input signal. If this error voltage is used to control the VCO frequency without the low pass filter indicated in Figure 8, the IF output signal should be essentially the same as the IF input signal, neglecting distortion, tracking errors, etc. The maximum rate at which the VCO needs to be varied for the passage of the signal is given by the highest frequency in the information signal. If random noise is present on the IF input signal, there will be spectral components higher than this at the mixer output. These may readily be removed by a low pass filter between the mixer and the VCO. If this is done, the IF output signal will be at a higher SNR than the IF input signal. For high SNR_{IF}, a detected signal from the output would contain less high frequency noise than a detected signal from the input prior to baseband filtering. After baseband filtering, both detected signals would have roughly the same SNR_{bb}. However, the threshold for the signal obtained by detecting the output will occur at a lower SNR_{IF}.

Notice that the output of the PLL is an IF signal. If the VCO frequency can be made to vary linearly with the control signal, a baseband signal can be obtained by differentiating the control signal. This is generally not the case, however, and the VCO signal is taken as the output. This signal may then be detected in a conventional FM detector.

With the advent of new and better voltage variable capacitors, a new generation of PLL demodulators may be in the making.

Much disagreement still exists on the analysis of the threshold reduction capability of the PLL demodulator. A rigorous, coherent analysis of the PLL demodulator, backed by experimentation, is badly needed, since the PLL is one of the most promising techniques for FM threshold reduction.

2.4 Tracking Filter

2.4.1 Introduction to the Tracking Filter

The tracking filter, like the PLL, is a straight forward approach to predetection filtering. It consists of a narrowband filter capable of following the instantaneous frequency of the input signal. Figure 9 shows a block diagram of a tracking filter of which the output is a filtered IF signal.

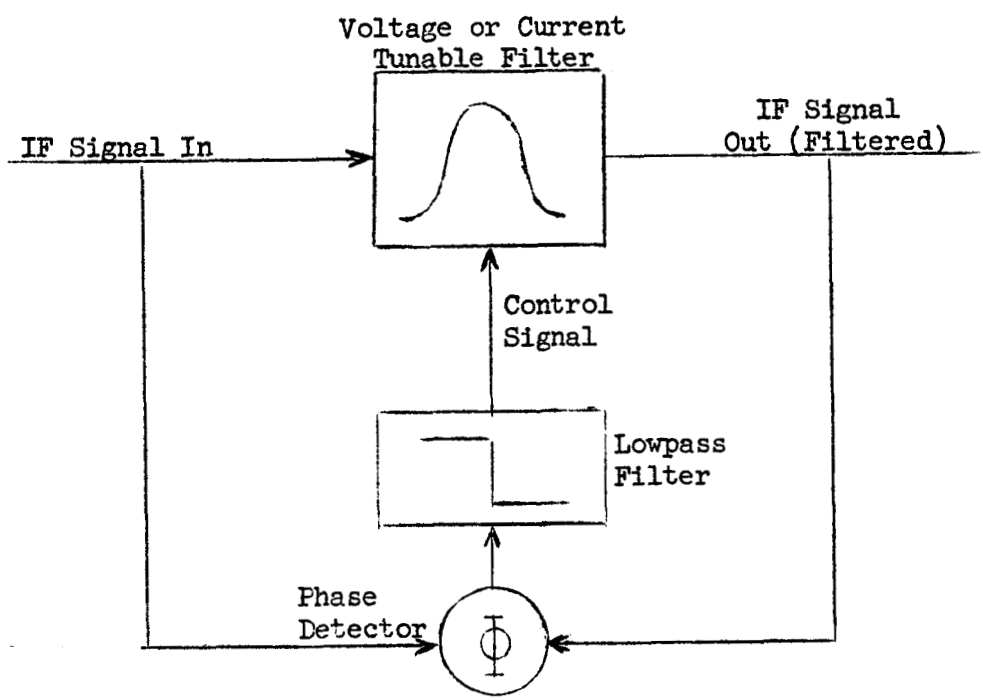

Figure 9. Block Diagram of a Tracking Filter

2.4.2 Discussion of the Tracking Filter

As pointed out earlier, an FM signal plus noise can be represented at a given instant in time by a single spectral component of a frequency equal to the time derivative of its phase. This frequency

will vary with time at a maximum rate given by the maximum baseband frequency. Thus, any variations faster than the highest frequency of the information signal, f_m, are caused by noise. If this spectral component is passed through a narrow filter, the output of the filter will be in phase with the input only when the center of the filter is of the same frequency as the spectral component. If samples of the input and output signals are fed into a phase detector, the phase detector output will be a voltage proportional to the phase error with zero output when the filter is at resonance.

If the phase detector output is used to control the tunable filter, without the lowpass filter indicated in Figure 9, the IF signal out will be essentially the same as the IF signal in neglecting time delays, ringing, etc. Since the maximum rate at which the filter needs to be tuned for passage of the signal is f_m, no frequencies are desired in the control signal higher than f_m. If random noise is present on the input signal, there will be spectral components of noise above f_m in the control signal. These components may be reduced by a lowpass filter between the phase detector and the filter. If this is done, the IF output signal will be at a higher SNR than the IF input signal. For high SNR_{IF}, a detected signal from the output would contain less high frequency noise than a detected signal from the input prior to baseband filtering. After baseband filtering, both detected signals would have roughly the same SNR_{BB}. However, the threshold for the signal obtained by detecting the output will occur at a lower SNR_{IF}.

The voltage or current tunable filter would probably be a single tuned circuit using either a current variable inductor or a voltage controllable capacitor (e.g., a Varicap).

This technique, previously not feasible because of the non-availability of reactive elements which can be electrically varied at a sufficiently high frequency, is now deserving of further analytical and experimental investigation.

3.0 EXPERIMENTAL RESULTS

3.1 Tracking Filter

3.1.1 Tube Model

To verify the tracking filter concept, it was decided to design and construct a tube model of the tracking filter. In order for the phase detector to give zero output, its two input signals must be in quadrature. To obtain this, it was decided to use a current sample from the inductor in the filter rather than a voltage sample from the output. The resonate frequency of the filter was controlled by Varicaps, voltage variable capacitors made by Philco. (Philco provided Varicaps up to 1,000 pf at 8 volts.) Figure 10 shows a block diagram and Figure 11 shows a schematic diagram of the bread-board model.

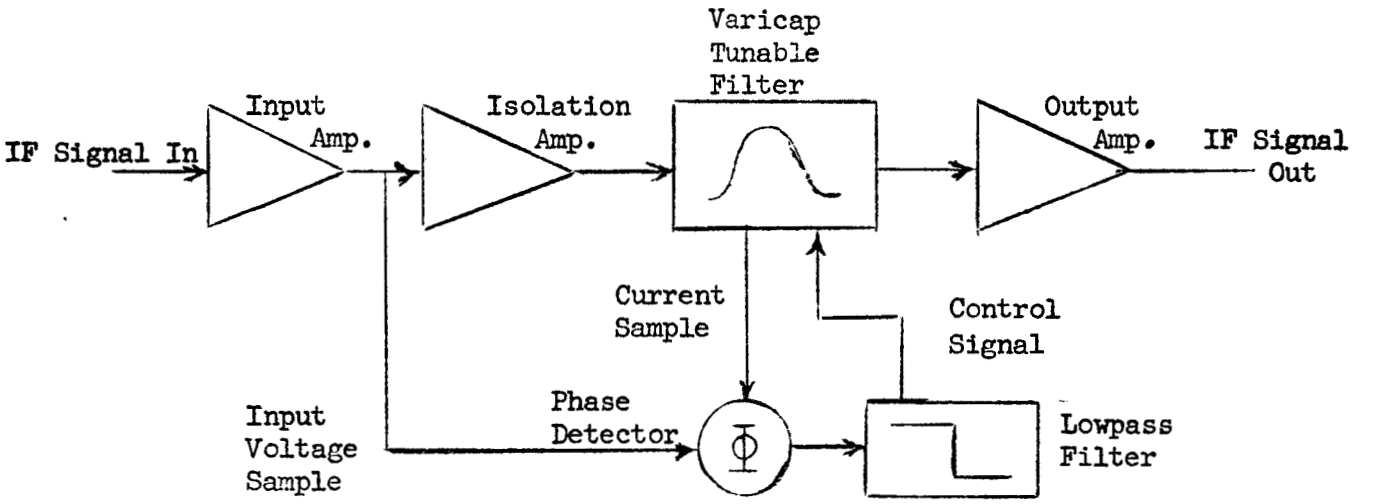

Figure 10. Block Diagram of the Tube Model of the Tracking Filter (Model No. TF-1)

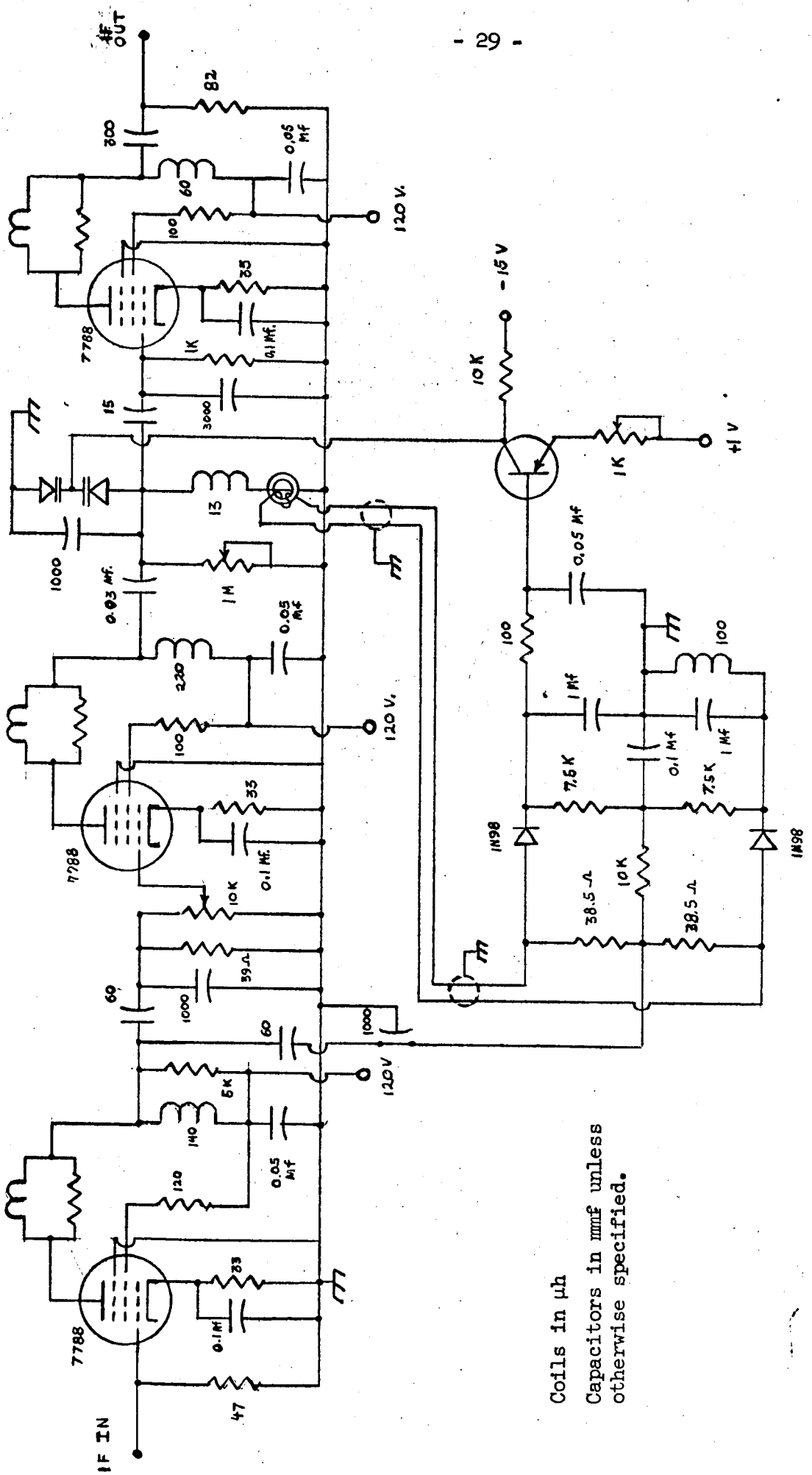

Figure 11. Schematic Diagram of Tracking Filter Model No. TF-1

The first stage is a low Q tuned amplifier. The input voltage sample for the phase detector is obtained via a capacitive divider at the output of this stage. The next stage drives the tank circuit and isolates the input voltage sample. The tank consists of a high Q toroidal coil in parallel with two series Varicaps connected back to back. The resonate frequency is changed by varying the voltage between the Varicaps. The current sample is obtained from a current transformer, enclosed in a Faraday shield, in series with the toroidal coil. The final stage isolates the tank from the output. A simple balanced phase detector is used to determine the error between the resonate frequency of the tank circuit and the instantaneous frequency of the input signal. The error voltage is filtered, amplified, and used to control the Varicaps. For simplicity, it was decided to use a solid state phase detector and control signal amplifier. The model is shown in Figure 12. Figure 13 shows the response of the system if the loop is opened by disconnecting the control signal. The solid line is the error signal from the phase detector. The other curve shows the bandpass of the system when it is not tracking.

To demonstrate the tracking nature of the filter, a 1.5 megacycle carrier was FM modulated to a 20 kilocycle deviation with a 10 kilocycle sine wave. Figure 14 shows the response of the model to this signal. The top curve is the output of the filter and the bottom curve is the control voltage. The amplitude modulation is caused by an inherent tracking error and could be reduced by increasing the loop gain.

Figure 15 depicts the loss of lock caused by sweeping the frequency too far. The signal used was a 1.5 megacycle carrier, FM modulated to a 65 kilocycle deviation with a 300 cycle sine wave. The top curve shows the filter output while the lower curve again shows the control signal.

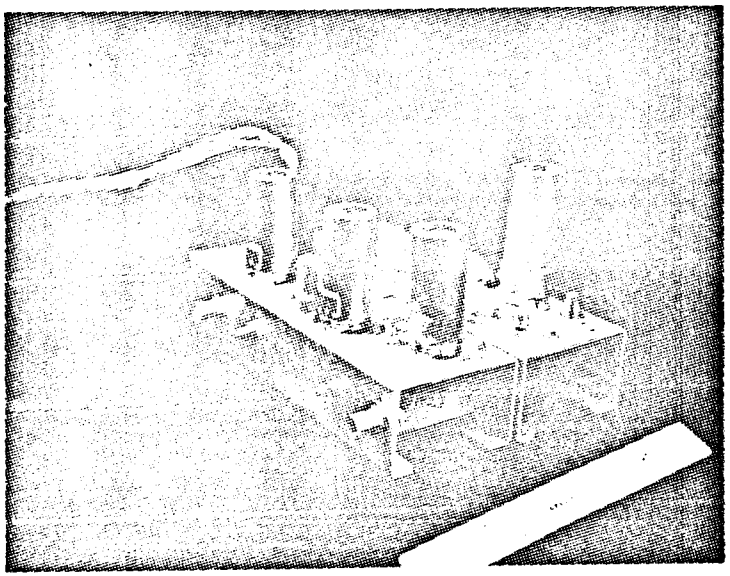

Figure 12.
Model No. TF-1 of the Tracking Filter

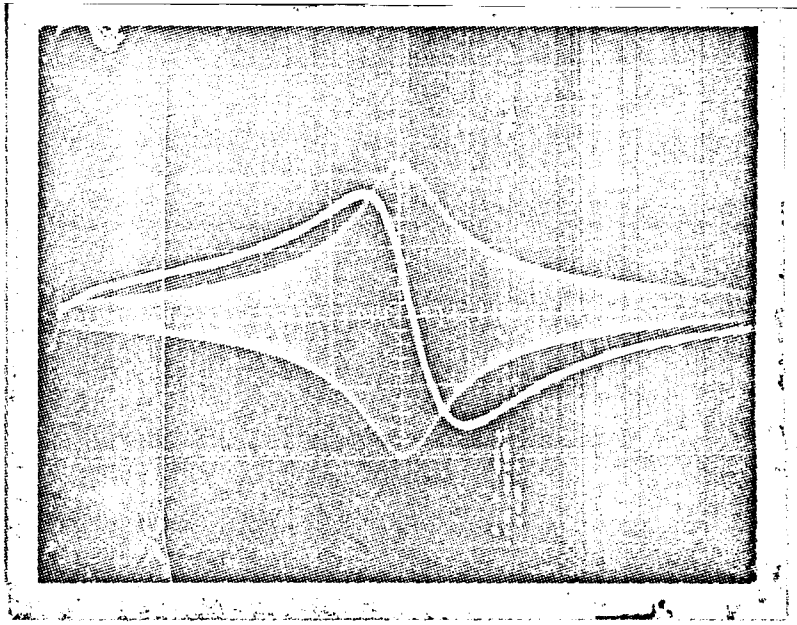

Figure 13.
Open Loop Response of Model No. TF-1

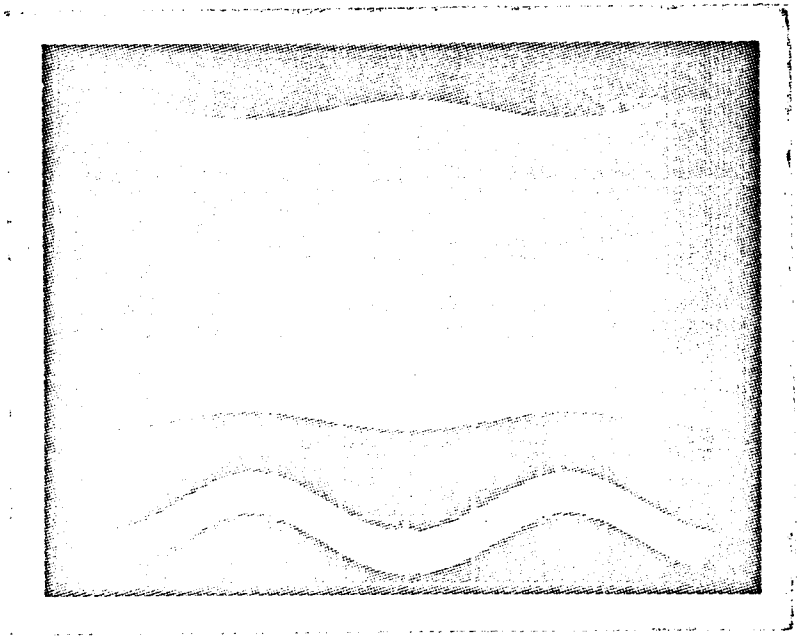

Figure 14.
Closed Loop Response of Model No. TF-1
While Tracking

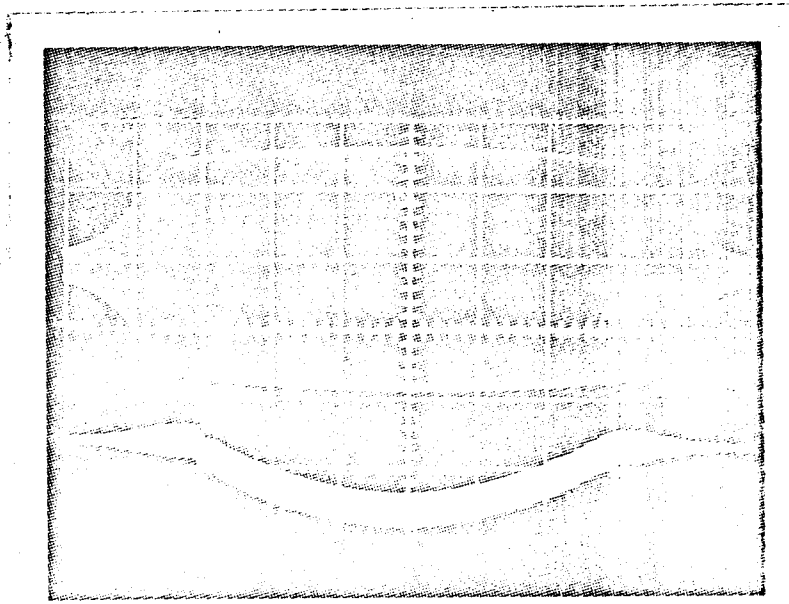

Figure 15.
Closed Loop Response of Model No. TF-1
Showing Loss of Lock at Band Edge

It was found that excessively high voltage was required across the tank circuit in order to keep the current sample above the Barkhausen noise inherent in the current transformer. However, large voltages made it difficult to keep the Varicaps properly biased and thus gave a distorted output. It was therefore decided to terminate tests on this model and begin design and construction of a transistor model. The new model would hopefully operate at lower signal levels in the tank, use samples from points which gave less noise problems, have a higher loop gain, and have provisions for obtaining a narrow bandwidth (higher Q) tank circuit.

3.1.2 Transistor Model

Figure 16 shows a block diagram of the transistorized tracking filter which was designed with the above points in mind.

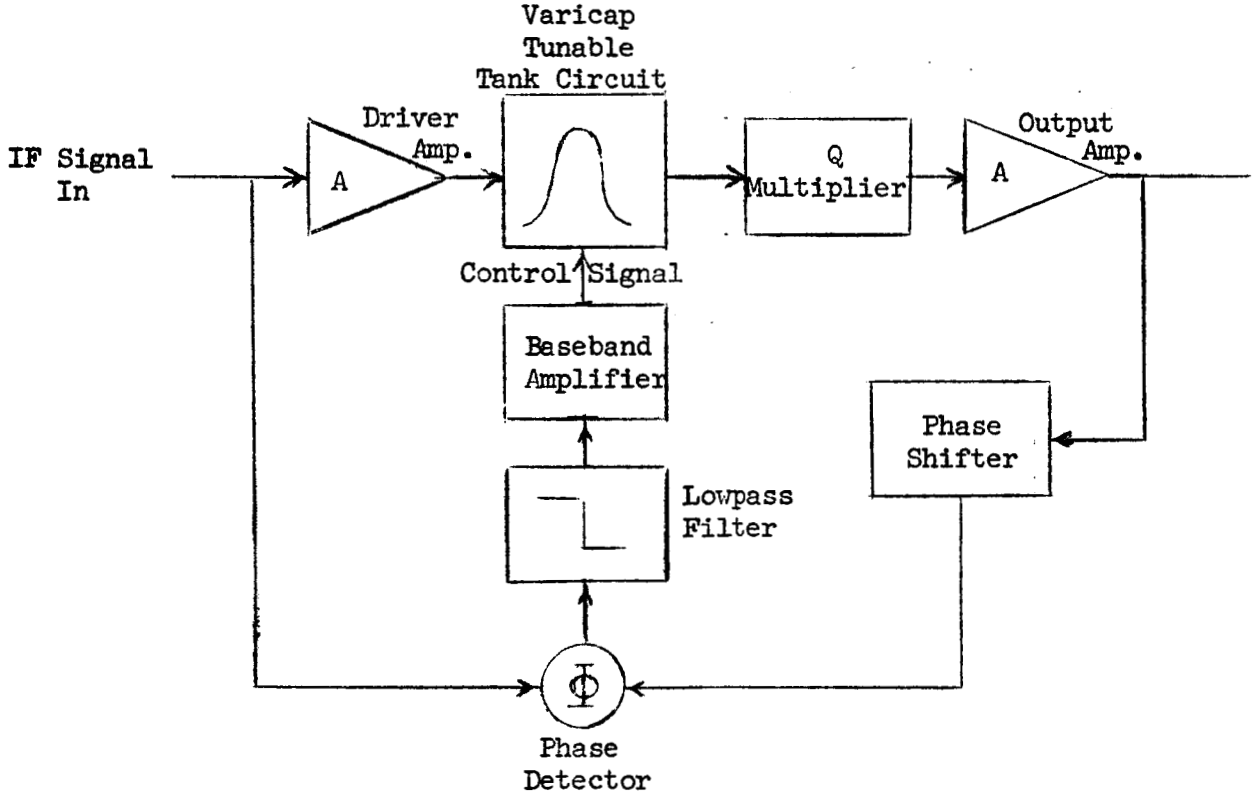

Figure 16. Block Diagram of Transistorized Tracking Filter (Model No. TF-2)

The high Q tank circuit is obtained through the use of a Q multiplier. An operational tracking filter would probably not require a Q multiplier, however, for experimentation, it was deemed desirable to be able to obtain extremely high Q's.

Note that the phase shifter must be designed so that the phase detector gives zero output when the tank is resonate at the input frequency. In this way, it is possible to compensate for time delays and phase shifts in the amplifiers.

Figure 17 shows a schematic diagram of the filter and Figure 18 shows the engineering model. The input stage is operated common base so that the tank appears to be driven from a current source. The tank again consists of a large toroidal coil in parallel with two series Varicaps connected back-to-back. The Varicaps, by Philco, are rated at 500 picofarads at 8 volts reverse bias. The Q of the tank can be adjusted by varying C_1 in the Q multiplier and R_1 in the tank circuit. Q's in excess of 1,500 were easily obtained using this scheme. The output amplifier consisted of a single emitter follower stage. For the phase detector, a simple mixer was selected. For the mixer to give the proper output, the phase shifter must be designed so that its output is in quadrature with the input voltage sample when the filter is at resonance. Proper design of the phase shifter could do more than match the quiescent center frequency of the filter to the carrier. It could also result in a compensation of changes in the amplifier phase shift with frequency and reduction of the tracking error which is inherent in any system of this sort.

It was decided to check out the filter first with the simple R-C phase shifter shown in Figure 11.

With the control signal disconnected, the open loop response is shown in Figure 19. The upper curve shows the filter response while it is not tracking and the lower curve shows the error voltage. Note that the error signal differs greatly from that shown in Figure 13, a much more desirable response. This deterioration is caused by too little phase shift in the phase shifter.

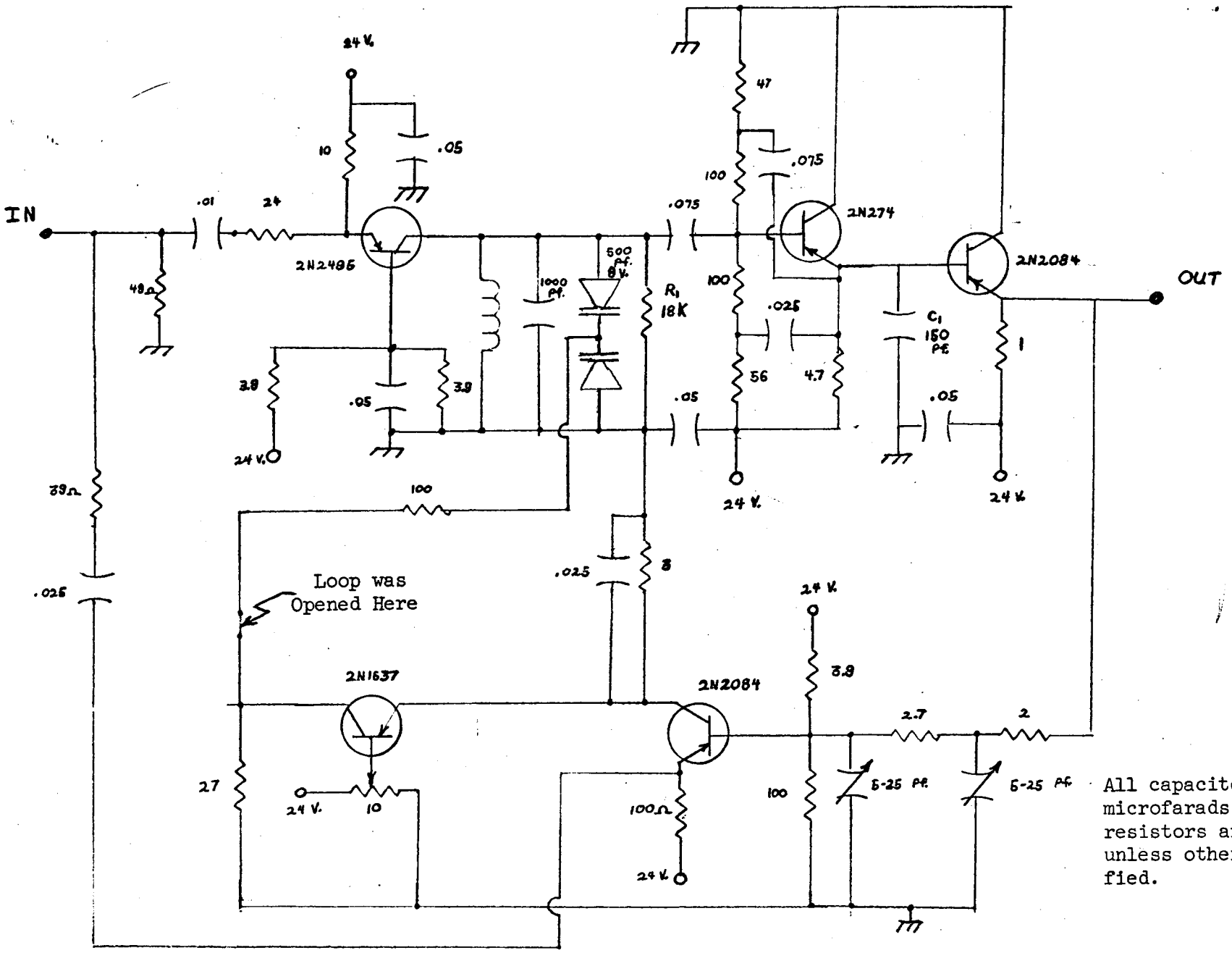

All capacitors are in microfarads and all resistors are in Kilohms unless otherwise specified.

Figure17. Schematic of the Tracking Filter Model TF-2

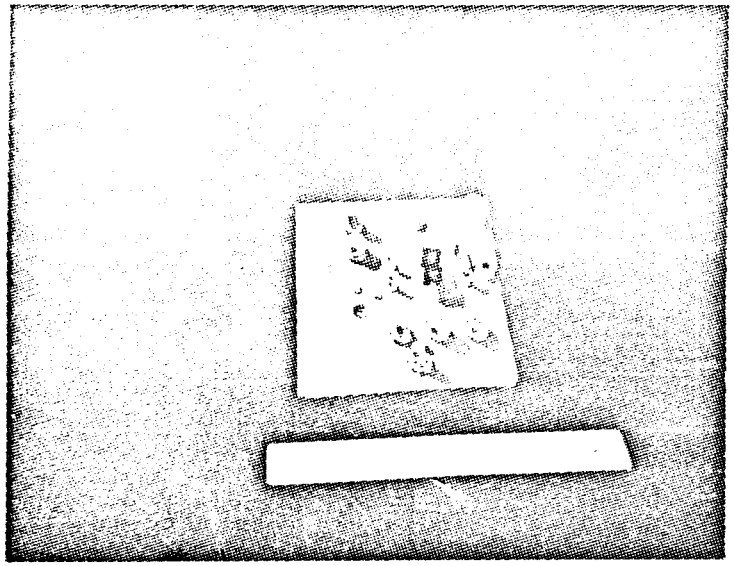

Figure 18.
Model TF-2 of the Tracking Filter

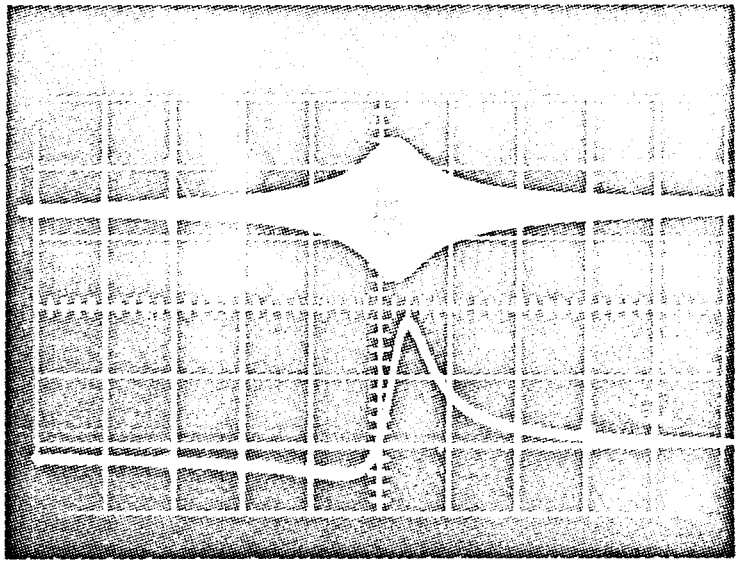

Figure 19.
Open Loop Response of Tracking Filter Model TF-2

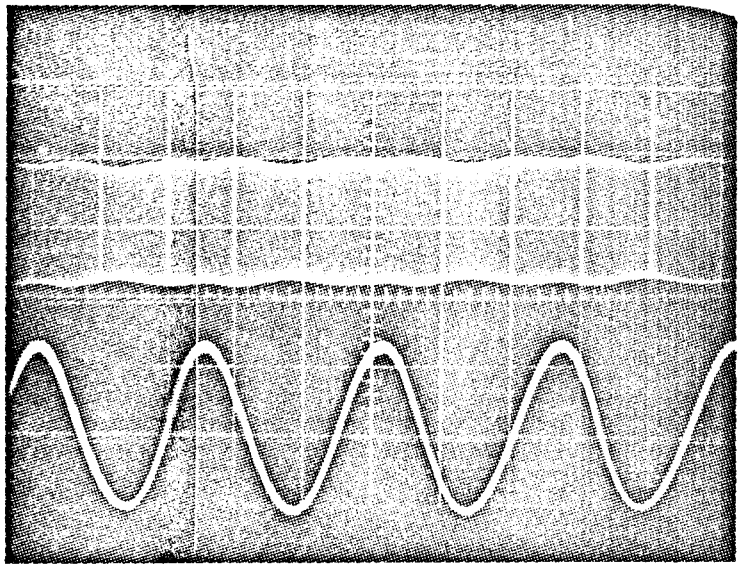

Figure 20.
Closed Loop Response of Model TF-2
While Tracking

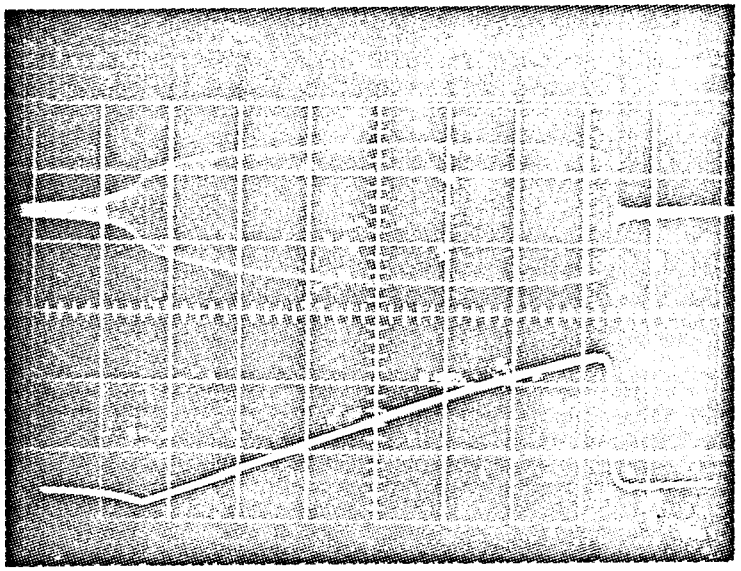

Figure 21.
Closed Loop Response of Response of
Model TF-2 Showing Loss of Lock at Band Edge

Figure 20 shows the closed loop response of the tracking filter to a 1.15 megacycle signal, FM modulated to a 15 kilocycle deviation by a 400 cycle sine wave. The top curve is the IF signal out of the filter. Variations in the tracking error can be seen in the form of amplitude modulation of this signal. The bottom curve is the control or error signal. Recall that if the resonate frequency of the filter varies linearly with the control voltage, the baseband signal, in this case the 400 cycle sinewave, can be obtained by differentiating the control signal.

Figure 21 shows the closed loop response of the filter as the input frequency is linearly swept past its passband. The upper curve is again the IF signal out and the lower is the control or error signal. As would be expected from the open loop response, the filter gradually comes into lock at the low frequency end and abruptly drops out of lock at the high frequency end. The amazingly linear response while in lock accounts for the very low distortion of the error signal in Figure 20.

The next step in the development of a good tracking filter would be to improve the phase shifter. Time did not permit this or any other additional experimentation or analysis to be done with the tracking filter. Although the tracking filter still looked very promising, it was necessary to defer additional work on it.

3.2 FCFL Demodulator

An experimental model of the frequency compressive feedback loop demodulator, the system which NASA expressed the most interest in, was designed and constructed. A block diagram of this model is shown in Figure 22.

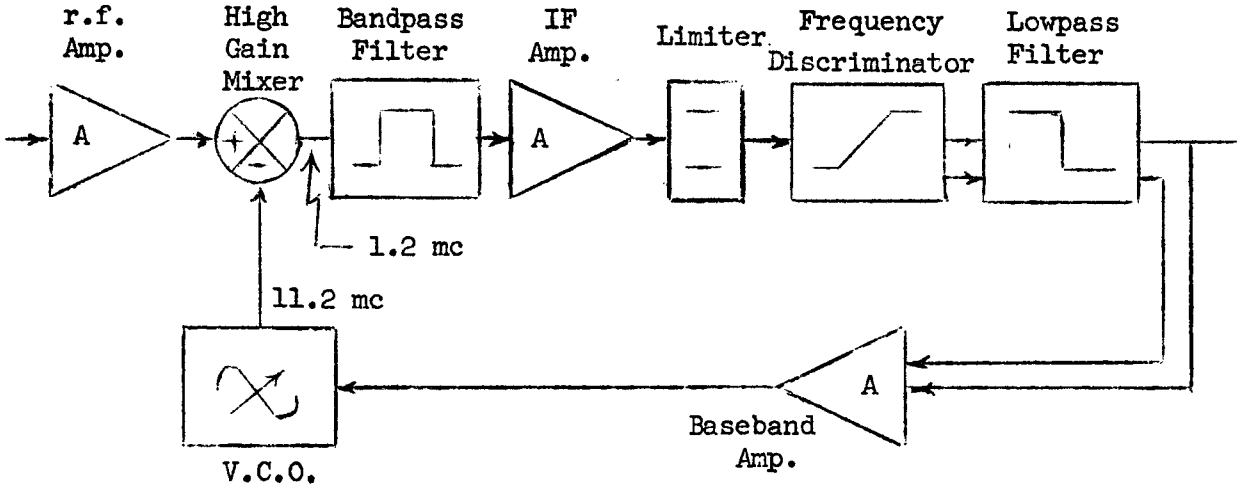

Figure 22. Block Diagram of the FCFL Demodulator Model

The loop must be designed for minimum time delay and maximum linearity to minimize the generation of new noise components. Figure 23 shows a schematic diagram of the model. All elements were kept simple to minimize time delay. The mixer gave a conversion gain of 40 db. The IF amplifier is an emitter follower, providing the low output impedance necessary to drive the simple diode limiter. The frequency discriminator provides a differential output and thus two lowpass filters were required, one from each output to ground. The outputs of filters are used to drive a differential baseband amplifier. A single ended output is taken from the differential amplifier in such a way that the gain may be varied even at d.c., but the quiescent output voltage will not change as the gain is varied. This permits direct coupling of the single ended baseband amplifier stage to the differential amplifier and then direct coupling the VCO to the single ended amplifier. Thus an AFC has essentially been built into the loop. The VCO uses Varicaps as the frequency determining elements.

Figure 24 shows the engineering model of the FCFL demodulator.

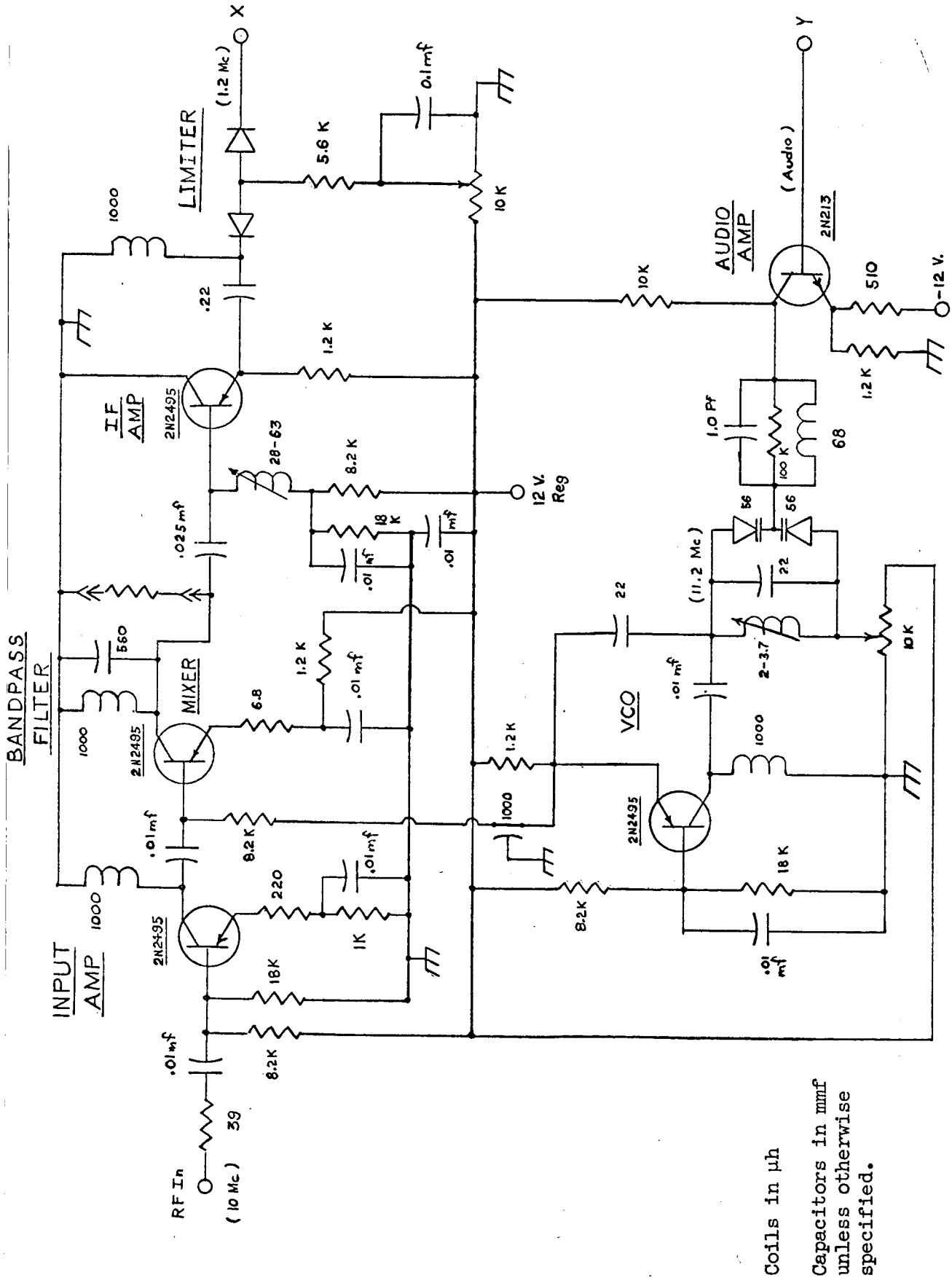

Figure 23 (a). Schematic Diagram of the FCFL Demodulator Model

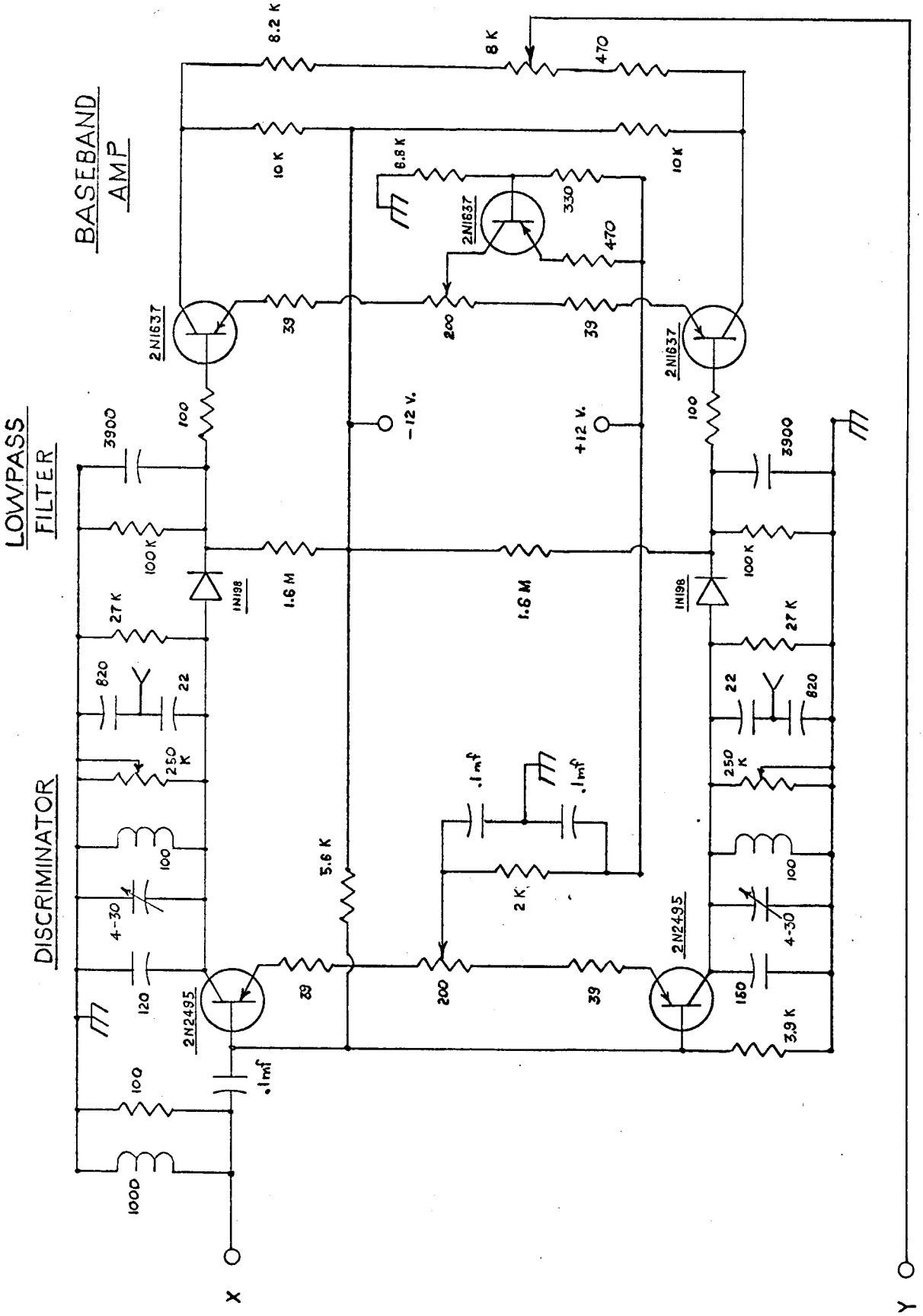

Figure 23 (b). Schematic Diagram of the FCFL Demodulator Model

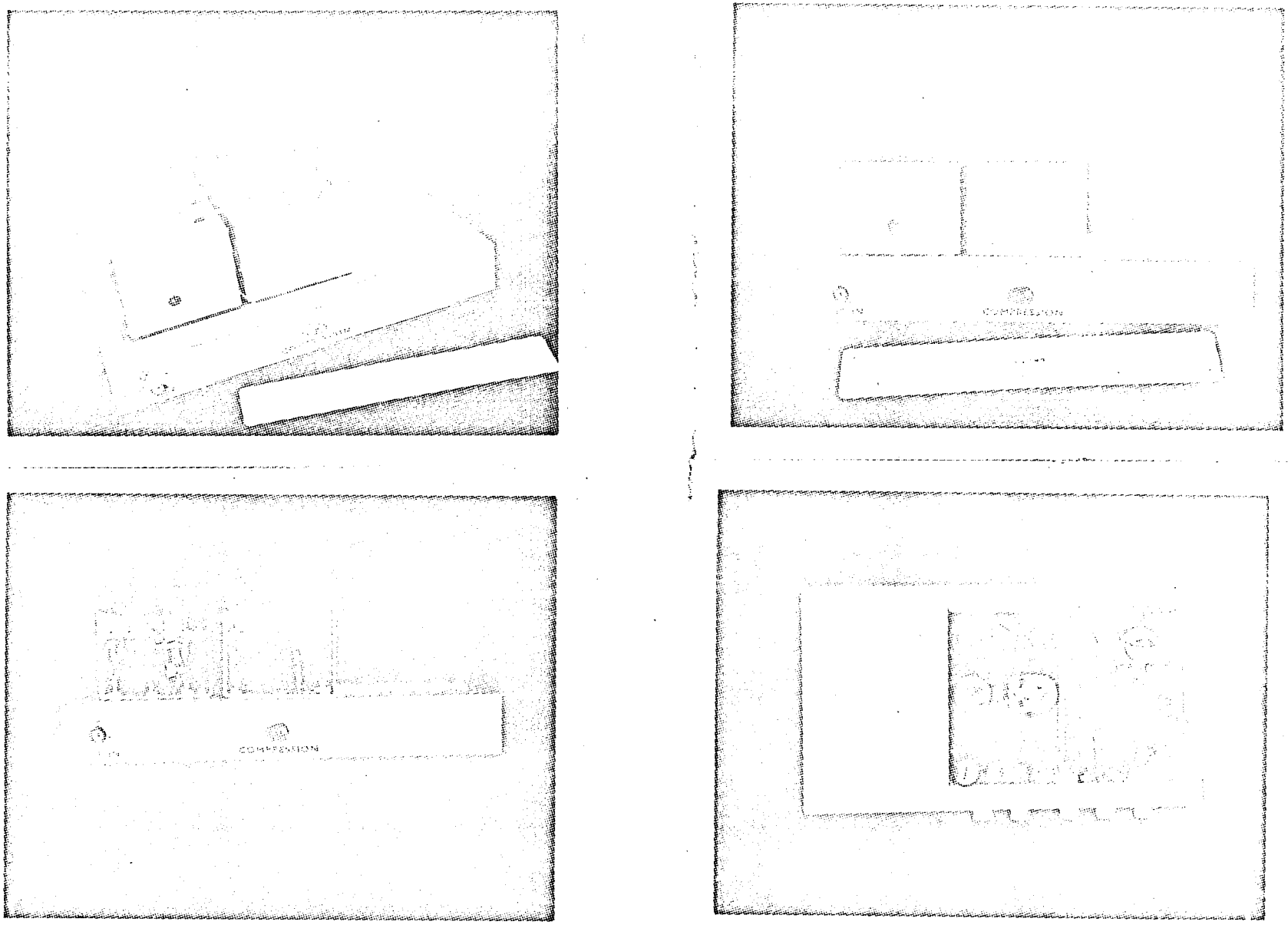

Figure 24. Engineering Model of the FCFL Demodulator

The FCFL demodulator that was constructed is capable of stable operation with up to 20 db of feedback around it. This can provide a modulation index reduction of up to 10 to 1. The bandwidth compression capabilities of the FCFL demodulator may be readily seen by comparing the signal spectrum at the input to the loop to that inside the loop before the discriminator. Figure 25 shows the spectrum of a typical sinusoidally modulated input signal. Figure 26 shows the signal inside the loop after compression. Comparison of the two spectral bandwidths of Figures 25 and 26 leads one to believe that if the loop bandpass filter were made just wide enough to pass the compressed signal, then an appreciable reduction of the noise bandwidth would be achieved. This would then result in a signal-to-noise ratio improvement before the discriminator and the desired threshold reduction would be realized. However, as discussed in Section 2.2.2 and further in Appendix V, if the loop bandpass filter is made just wide enough to pass the compressed signal, this will not particularly reduce the noise bandwidth before the discriminator after feedback is applied. Figures 27 and 28 illustrate the effects of feedback on the noise bandwidth preceding the discriminator. Figure 27 shows the open loop carrier-plus-noise spectrum at the discriminator input. Figure 28 shows the effects of a large amount of feedback on the noise spectrum at the discriminator input. This increased bandwidth due to feedback is still very much in evidence even after lowpass filtering in the loop. Figure 29 shows the open and closed loop baseband response for two values of loop bandpass filter bandwidth. The FCFL demodulator characteristics presented in Figures 25 through 29 graphically illustrate the inherent limitations of the FCFL approach to FM threshold reduction. While the FCFL demodulator does provide a considerable reduction in the signal bandwidth, it makes very inefficient use of this narrowband signal because of the limited filtering possible inside the loop and the loop bandwidth expansion inherent in all negative feedback loops. It is obvious that the amount of threshold improvement predicted for the idealized FCFL demodulator is not attainable. As a matter of fact, if care is not exercised in the design of the FCFL demodulator, not only

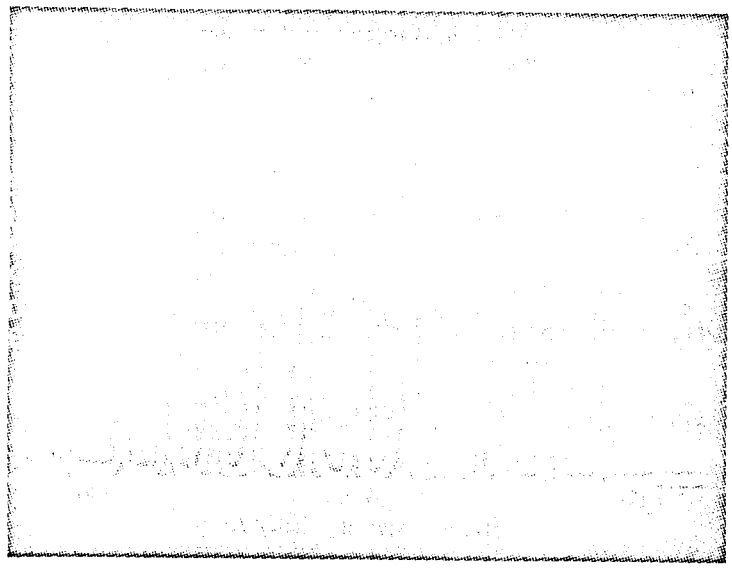

Figure 25. Spectrum of an Input Signal to an FCFL

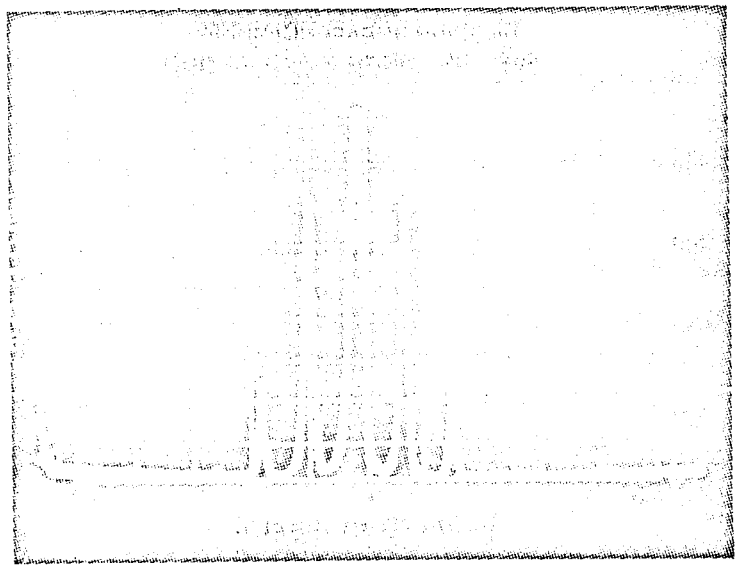

Figure 26. Spectrum of a Discriminator Input to an FCFL

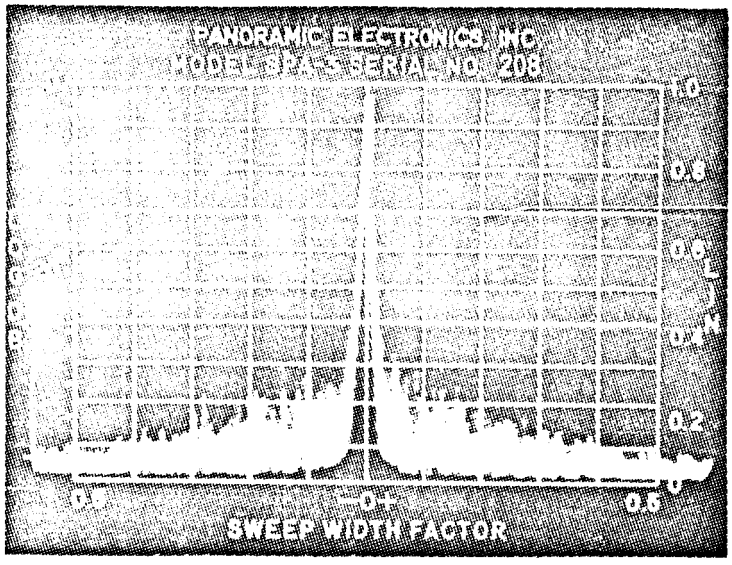

Figure 27. Open Loop Carrier-Plus-Noise Spectrum

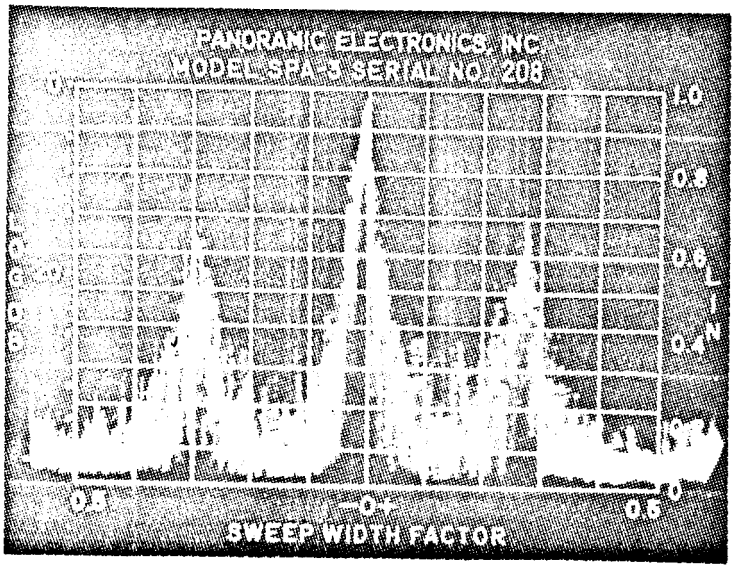

Figure 28. Closed Loop Carrier-Plus-Noise Spectrum

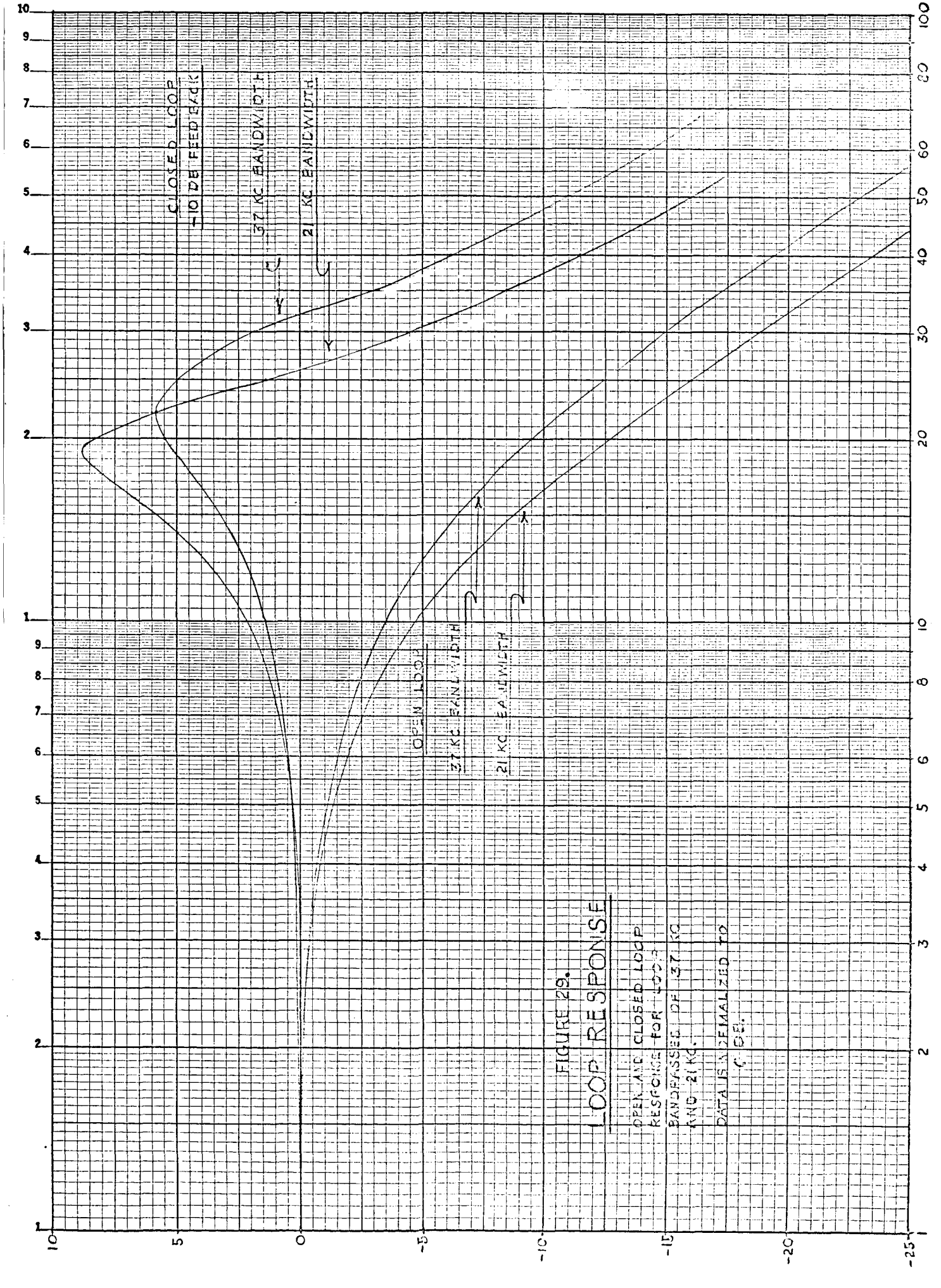

FIGURE 29.

LOOP RESPONSE

OPEN AND CLOSED LOOP RESPONSE FOR LOOP BANDPASSED OF 37 KC AND 21 KC.

DATA IS NORMALIZED TO 0 DB.

will the IF signal-to-noise ratio at which the threshold occurs be appreciably reduced, but the overall system performance may be deteriorated.

The linear tracking capability of the engineering model FCFL demodulator is illustrated in Figures 30 and 31. These figures show the open and closed loop responses respectively when the input signal is linearly swept over 300 kc. The solid trace is the VCO input signal; the other is the loop bandpass filter response to the swept input signal. The abrupt rise at the low frequency end of the response in Figure 31 is caused by forward biasing of the VCO Varicaps. Under normal operation, the loop operates only over a small portion of this characteristic.

Before performance data could be taken on the FCFL demodulator, it was necessary to construct a baseband filter which would take advantage of the FM improvement capabilities of the loop discriminator. As illustrated in Figure 29, the single pole loop lowpass filter does not provide a desirable baseband characteristic even under open loop conditions. The response characteristics of the baseband filter, which is used external to the loop, is shown in Figure 32. Its schematic is shown in Figure 33.

It was also necessary to construct a 10 mc IF amplifier with the capability of providing at least two different noise bandwidths so comparative data could be taken on loop performance. The test setup is diagramed in Figure 34. It is necessary to make the input signal and noise measurements at a point well isolated from the VCO signal or the data taken will be adversely affected by oscillator feedthrough, especially at high SNR's. It is also desirable to take all data with the VTVM at one point so that network corrections are not necessary as the VTVM is moved about. For this reason, the SNR_{IF} is measured at the output of the 10 mc IF amplifier. This poses no problem for closed loop measurements, for the noise bandwidth at this point is the desired one. However, when taking open loop data, the noise bandwidth at the discriminator input is determined by both the 10 mc IF amplifier and the loop Bandpass Filter. It is thus necessary to determine a factor which will correct the SNR, as measured at the 10 mc IF output, for the additional selectivity

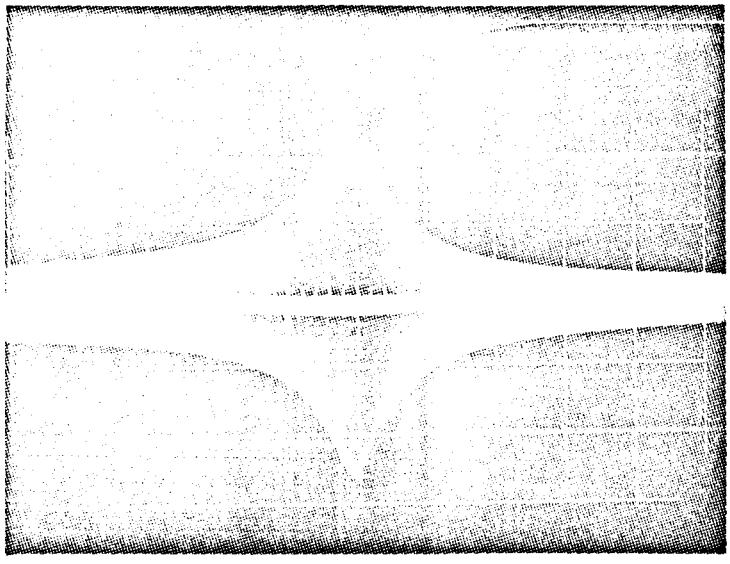

Figure 30. Open Loop Swept Frequency Response

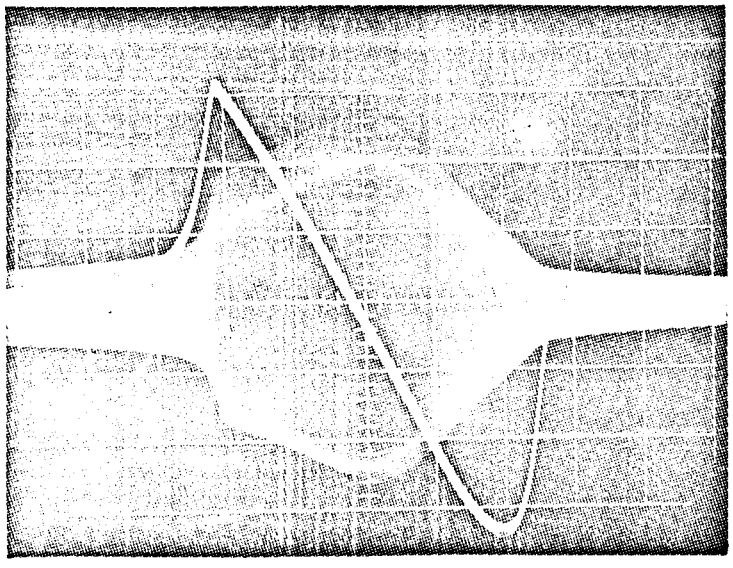

Figure 31. Closed Loop Swept Frequency Response

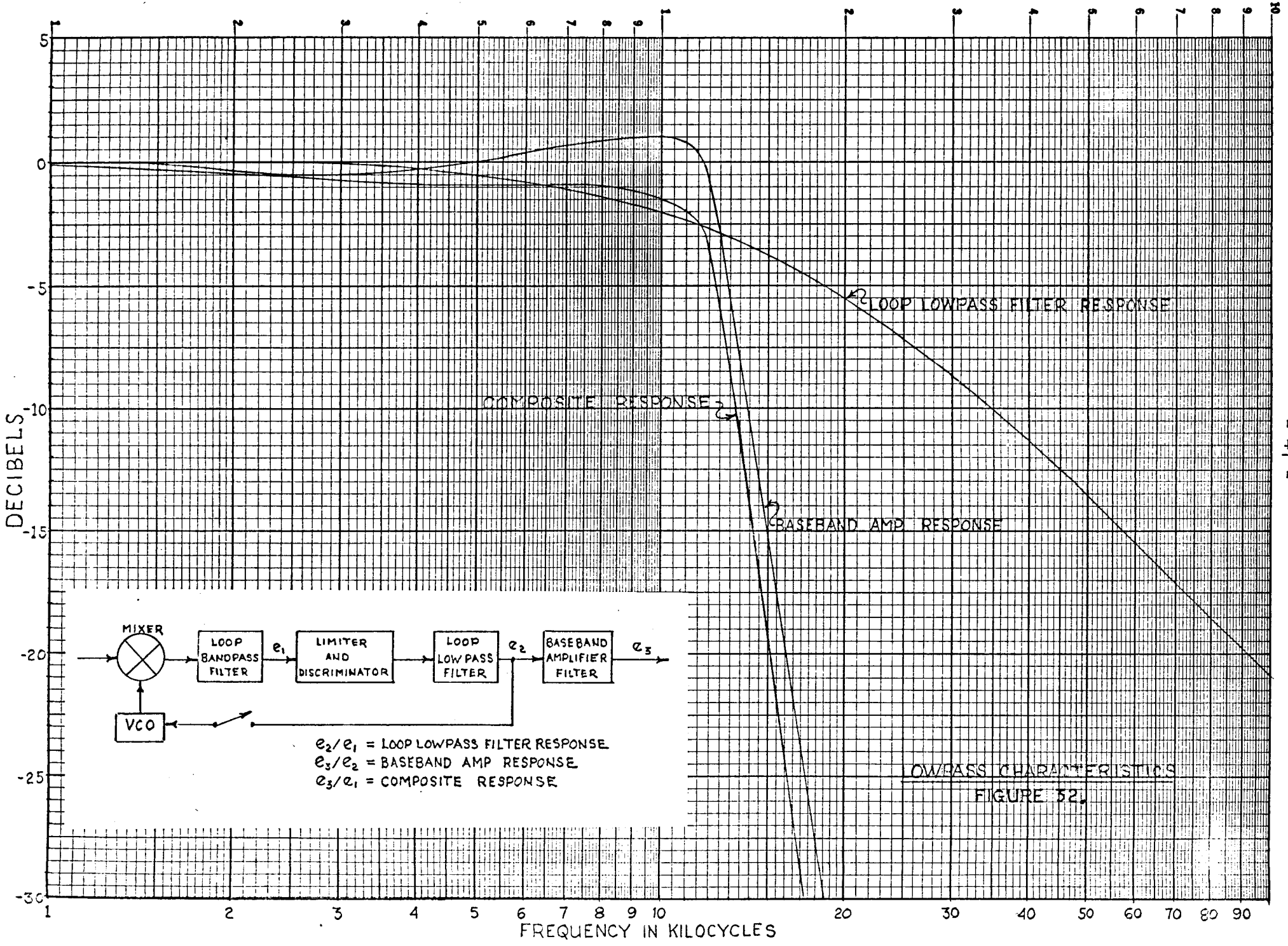

LOWPASS CHARACTERISTICS

FIGURE 52.

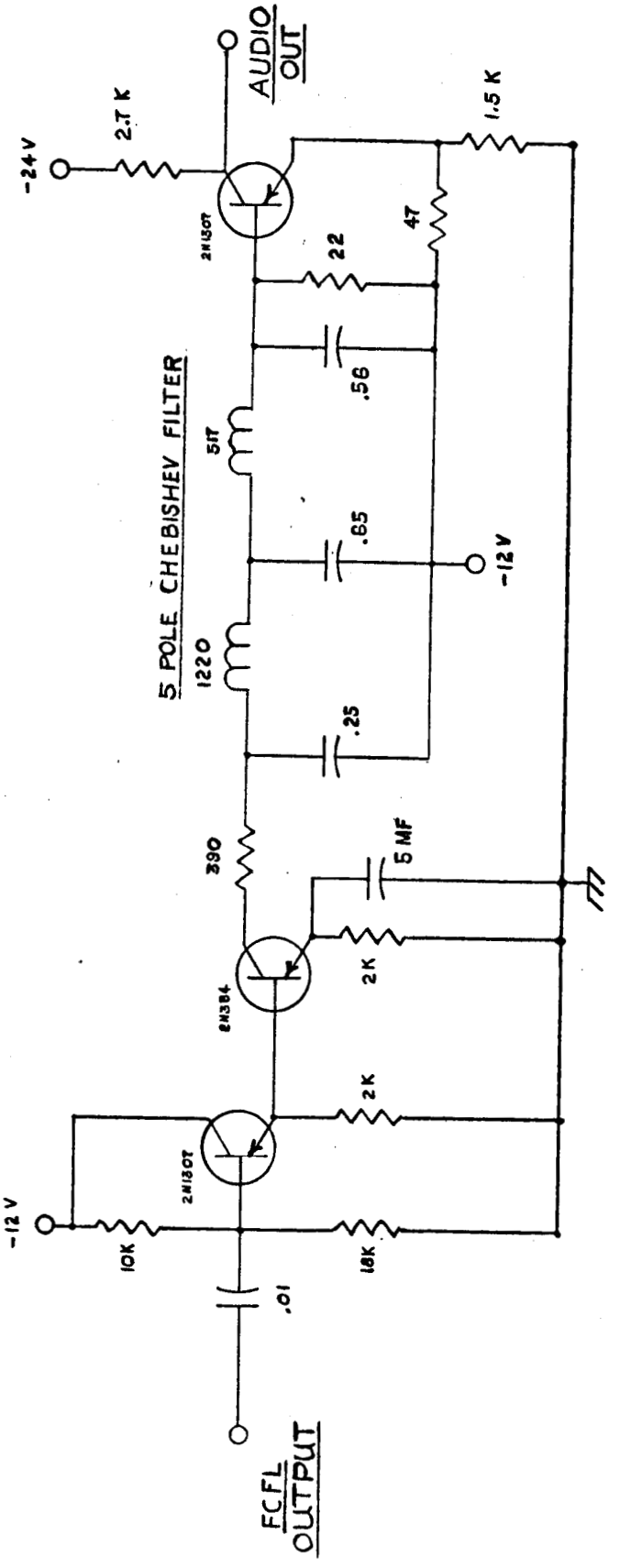

Figure 33. Schematic Diagram of Baseband Amplifier Filter

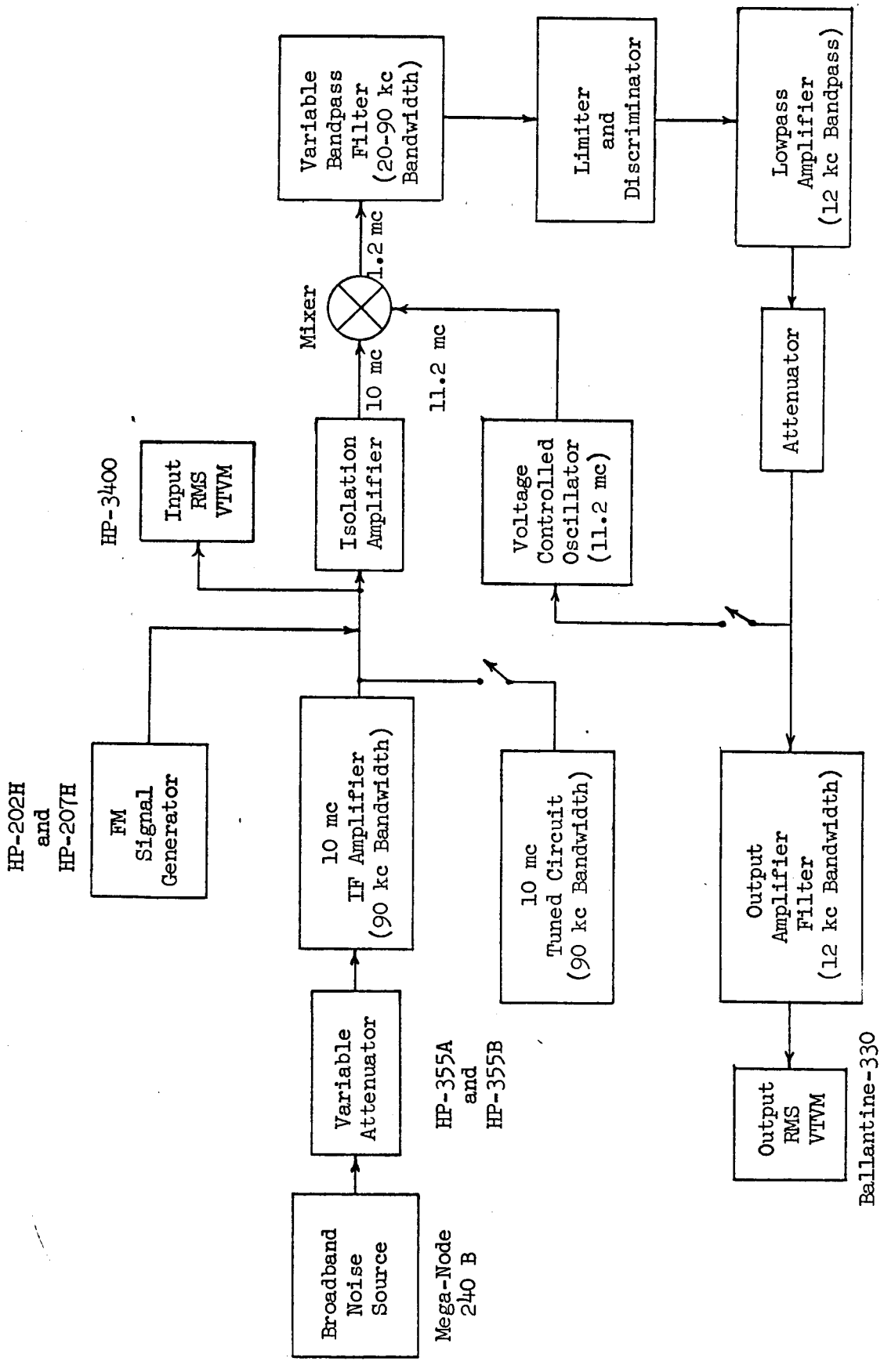

Figure 34. Test Setup

afforded by the loop Bandpass Filter, in the open loop case. By making comparative measurements at the two points, at low SNR, where the VCO feedthrough is almost negligible, it was determined that the correction factor was essentially the ratio of the 3 db bandwidths measured at the two points.

A modulation index of 1.2 was chosen as the value at which comparative SNR data would be taken. This represents a typical carrier modulation index value for the Apollo data system as outlined in the Specification for Signal Data Demodulator System (GSFC-TDS-RFS-226).

The objectives of the following data collection procedure is to obtain accurate, true RMS values for the input RF carrier voltage and the output baseband voltage. These quantities must be measured without noise or sufficiently above the noise so that they may be used to calculate the reference input and output signal powers, respectively. It is then necessary to obtain the true RMS noise output with an input carrier and the true RMS input noise without carrier present over a wide range of input noise power. The SNR_{IF} is then 20 log of the ratio of the RMS input carrier to the input noise and the SNR_{BB} is 20 log of the ratio of the RMS reference baseband output signal to the output noise. The input and output signal and noise voltages must be measured at the same points in their respective circuits so that these signal-to-noise power ratios may be calculated without consideration to the circuit impedance levels.

The feedback loop was opened and the loop Bandpass Filter was set at a 90 kc bandwidth. The FM Signal Generator was set to provide a 10 mv FM signal at 10 mc, deviated 12 kc by a 10 kc sinusoidal baseband signal. The Noise Source Attenuator was set at maximum attenuation to provide the highest possible input SNR. The output signal level was then recorded from the Output VTVM for reference purposes. The modulation was turned off at the FM Signal Generator for the rest of the measurements. The Noise Source attenuation was next reduced until a noticeable change was observed in the output noise and the output noise level was recorded. The input signal carrier was then removed and the input noise level was recorded. The input signal carrier was then replaced and the

Noise Source attenuation was reduced 1 db. This procedure was repeated until data had been obtained well beyond the discriminator threshold. The curve labeled "Open Loop (M = 1.2)" of Figure 35 shows a typical SNR transfer characteristic as calculated from data obtained through this procedure. Next, the loop Bandpass Filter bandwidth was reduced to 20 kc, and the input modulation index was set at 0.6. The procedure was then repeated to obtain the curve labeled "Open Loop (M = 0.6)" of Figure 35.

The loop was then closed and 12 db of feedback applied. The loop Bandpass Filter was left at 20 kc bandwidth and the modulation index set at 1.2. A 10 mc, 90 kc wide, tuned circuit was then inserted at the 10 mc IF Amplifier output to provide essentially the same 60 kc noise bandwidth at the input to the FCFL demodulator as was previously present at the discriminator input in the open loop case. The above procedure was then repeated and the curve labeled "12 db Feedback (M = 1.2)" was obtained.

To check agreement of the test results with the expression derived in Section 2.1.2 for the SNR transfer characteristic of the conventional demodulator, the test conditions are plugged into equation 16. The baseband bandwidth is 12 kc for all tests. For a modulation index of 1.2, the IF bandwidth is 60 kc and for a modulation index of 0.6, it is 20 kc. The transfer relationship above threshold for these two cases are:

For M = 1.2

$$SNR_{bb}(db) = SNR_{IF} + 10.3 \text{ db}$$

For M = 0.6

$$SNR_{bb}(db) = SNR_{IF} - 0.46 \text{ db}.$$

The curves labeled "Predicted" of Figure 35 are plots of these relations.

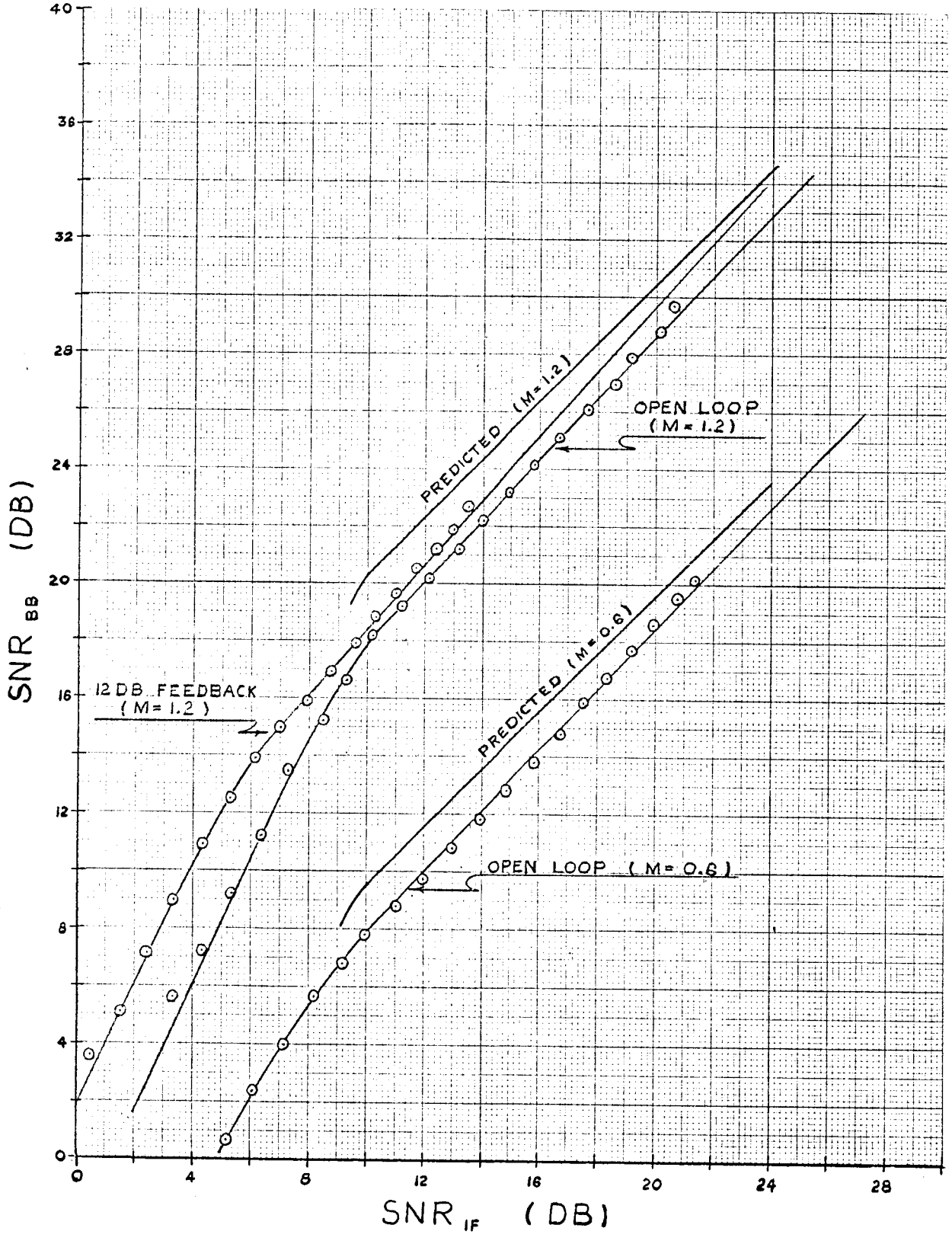

Figure 35. FCFL Performance Data

4.0 CONCLUSIONS

A great deal may be concluded about the performance of a frequency demodulator, and an FCFL demodulator in particular, from Figure 35. The open loop data appears to agree relatively well with the predicted results. The SNR_{bb} data is, in both cases, always less than the predicted. This is undoubtedly due in part to noise products generated in the mixer. This assumption is born out to some extent by the fact that the data approaches the predicted values as the SNR improves.

The open loop data also appears to verify the 10 db, conventional demodulator threshold point predicted in Section 2.1.2, and the fact that the threshold is the same regardless of the modulation index.

It was pointed out in Section 2.2.1 that the addition of feedback to the demodulator should reduce the signal and noise by the same amount, thus above threshold there should be no difference between the two. The data of Figure 35 agrees very closely with this theory. The slight difference observed is most likely due to a variation between the noise bandwidth preceding the frequency discriminator in the open loop case and the noise bandwidth into the FCFL in the closed loop case. The variation noted in the slope of the two curves above threshold is most probably due to additional noise products generated in the mixer when the loop is closed.

The noise bandwidth at this frequency discriminator is 60 kc in the open loop case and 20 kc in the closed loop case. From the idealized FCFL model, the threshold improvement would then be predicted to be approximately three-to-one or 4.8 db. The data of Figure 35 shows the closed loop threshold to lie between 6 db and 7 db. This is an actual improvement of only about 3.5 db. This inability of the FCFL demodulator to achieve the improvement predicted from the idealized model is due, in the most part, to the increased noise bandwidth inside the loop. The threshold reduction capability of the FCFL demodulator could probably be improved if a design criterion could be arrived at that would optimize the loop bandpass and lowpass bandwidths for the amount of feedback used.

The amount of improvement that could be gained by this optimization is not expected to be very drastic. The threshold reduction in higher modulation index systems employing greater amounts of feedback might be expected to be much more dramatic. However, the amount of frequency compression possible in the FCFL demodulator is a function of the amount of feedback that is applied. Because of the delays inherent in presently known limiter, discriminator, and voltage controlled oscillator circuits, the amount of feedback it is possible to apply and still maintain an unconditionally stable system is very definitely limited. This limit appears to be somewhere in the vicinity of 20 db; and, at values above 15 db, exact circuit alignment becomes very critical to stability.

It is concluded from the investigation that the FCFL demodulator's inefficient use of its compressed signal frequency spectrum, and the loop stability criterion, place very restrictive limits on its threshold reduction capabilities. Predetection filtering techniques which are not so susceptible to circuit delays and which could make more efficient use of their bandwidth reduction capabilities, by keeping the control loop outside the normal signal path, appear to have a great deal more promise. Two possible techniques which seem to meet these requirements are the Frequency-Tracked-Filter and the Phase-Locked-Loop which are discussed briefly in this report. These techniques have an inherent advantage over the FCFL demodulator in that they do not require nearly as complex circuitry and they are not plagued by the severe problem of noise bandwidth expansion. They have an additional practical advantage in that they can be inserted in an existing receiver system without major modifications to the system. No experimental work was conducted on the PLL demodulator in the course of this investigation. It is pointed out, however, that with the advent of new and better Varicaps, voltage controllable capacitors, and the possibility of employing improved lowpass filtering techniques could lead to a greatly improved generation of PLL demodulators.

Two rather crude models of the Tracking Filter were built, one tube model and one transistor model. While preliminary tests indicated that this technique showed great promise, lack of time made it necessary to defer further experimentation. This technique, when perfected, would have many applications in addition to FM demodulation.

BIBLIOGRAPHY

1. John R. Carson, T. C. Fry, "Variable Frequency Electric Circuit Theory with Application to the Theory of Frequency Modulation," Bell System Technical Journal, October, 1937.

2. H. Roder, "Effects of a Tuned Circuit Upon an FM Signal," Proceedings of the IRE, December, 1937.

3. M. G. Crosby, "Frequency Modulation Noise Characteristics," Proceedings of the IRE, April, 1937.

4. John R. Carson, "Frequency Modulation Theory of Feedback Receiving Circuits," Bell System Technical Journal, July, 1939.

5. J. G. Chaffee, "The Application of Negative Feedback to Frequency Modulation Systems," Bell System Technical Journal, July, 1939.

6. Stanford Goldman, "Frequency-Modulation Noise and Interference," Electronics, August, 1941.

7. M. W. Bode, "Network Analysis and Feedback Amplifier Design," D. Van Nostrand Company, New York, 1945.

8. S. O. Rice, "Statistical Properties of a Sine Wave Plus Random Noise," Bell System Technical Journal, January, 1948.

9. C. E. Shannon, "Communication in Presence of Noise," Proceedings of the IRE, January, 1949.

10. C. E. Shannon, "Recent Developments in Communication Theory," Electronics, April, 1950.

11. R. M. Wilmotte, "Reduction of Interference in FM Receivers by Feedback Across the Limiter," Proceedings of the IRE, January, 1952.

12. R. C. Boonten, Jr., "The Analysis of Non-Linear Control Systems with Random Inputs," Proceedings of Non-Linear Circuit Analysis, Polytechnic Institute of Brooklyn, New York, 1953.

13. H. S. Black, "Modulation Theory," D. Van Nostrand Company, New York, 1953.

14. J. Dujundji, "Envelopes and Pre-Envelopes of Real Wave Forms," Transactions on Information Theory, March, 1958.

15. D. K. Weaver, Jr., "Quadrature Signal Functions and Applications," ERL Report, Montana State College, Bozeman, Montana, December, 1958.

16. E. J. Baghdady, "FM Interference and Noise Suppression Properties of the Oscillating Limiter," IRE National Convention Record, 1959.

17. M. Morita, S. Ito, "High Sensitivity Receiving Systems for Frequency Modulated Waves," IRE International Convention Record, 1960.

18. E. D. Martin, "Threshold Improvement in an FM Subcarrier System," Transactions on Space Electronics and Telemetry, March, 1960.

19. W. A. Edson, "Noise in Oscillators," Proceedings of the IRE, August, 1960.

20. E. A. Ohm, "Receiving System (Echo)," Bell System Technical Journal, July, 1961.

21. C. L. Ruthroff, "FM Demodulators with Negative Feedback (Echo)," Bell System Technical Journal, July, 1961.

22. E. J. Baghdady, "A Technique for Lowering the Noise Threshold of Conventional Frequency, Phase, and Envelope Demodulators," Transactions on Communications Systems, September, 1961.

23. J. J. Spilker, "Threshold Improvement in an FM Subcarrier System," Transactions on Space Electronics and Telemetry, June, 1961.

24. J. J. Spilker, "Threshold Comparison of Phase Lock, Frequency Lock, and Maximum Likelihood Types of FM Discriminators," IRE Wescon, 1961.

25. J. S. Smith, "Impulse Noise Reduction in Narrow-Band FM Receivers: A Survey of Design Approaches and Compromises," Transactions on Vehicular Communications, August, 1962.

26. David Slepian, "The Threshold Effect in Modulation Systems that Expand Bandwidth," Transactions on Information Theory, September, 1962.

27. L. H. Enloe, "Decreasing the Threshold in FM by Frequency Feedback," Proceedings of the IRE, January, 1962.

28. E. J. Baghdady, "The Theory of FM Demodulation with Frequency Compressive Feedback," Transactions on Communications Systems, September, 1962.

29. R. E. Heitzman, "A Study of Threshold Requirements of FMFB Receivers," Transactions on Space Electronics and Telemetry, December, 1962.

30. J. J. Spilker, "Analysis of the FM Discriminator with Frequency Feedback," Proceedings of the IEEE, January, 1963.

31. P. W. Dippolito, L. B. Arguimbau, "A Double Balanced Modulator," Proceedings of the IEEE, March, 1963.

32. E. J. Baghdady, "Dynamics of a Signal-Squelched Oscillating Limiter," Proceedings of the IEEE, March, 1963.

33. J. J. Downing, "Threshold Suppression by FM Feedback," Proceedings of the IEEE, February, 1963.

34. J. A. Develet, Jr., "A Threshold Criterion for Phase-Locked Demodulation," Proceedings of the IEEE, February, 1963.

35. E. J. Baghdady, "On the Noise Threshold of Conventional FM and PM Demodulators," Proceedings of the IEEE, September, 1963.

36. L. H. Enloe, C. L. Ruthroff, "A Common Error in FM Distortion Theory," Proceedings of the IEEE, May, 1963.

37. F. L. H. M. Stumpers, "Theory of Frequency-Modulation Noise," Proceedings of the IRE, New York, September, 1948.

38. W. B. Davenport, Jr., W. L. Root, "Random Signals and Noise," McGraw Hill, New York, 1958.

39. D. L. Schilling, J. Billig, "A Comparison of the Threshold Performance of the Frequency Demodulator Using Feedback and the Phase Locked Loop," Polytechnic Institute Report, Brooklyn, New York, February 28, 1964.

40. M. Rosenblatt, "Random Signals and Noise," Wiley, New York, 1963.

41. E. J. Baghdady, "Theoretical Comparison of Exponent Demodulation by Phase-Lock and Frequency-Compressive Feedback Techniques," IEEE International Convention, 1964.

42. P. Frutiger, J. S. Vogel, "Demodulation of FM Signals at High Noise Levels," Proceedings of the IEEE, November, 1963.

43. E. J. Baghdady, "Theory of Feedback Around the Limiter," IRE National Convention Record, 1957.

44. W. R. Bennett, "Methods of Solving Noise Problems," Proceedings of the IEEE, May, 1956.

45. J. R. Pierce, "Physical Sources of Noise," Proceedings of the IEEE, May, 1956.

46. C. L. Ruthroff, "Design and Performance of a Broad-Band FM Demodulator With Frequency Compression," Proceedings of the IEEE, December, 1962.

47. A. S. Gladwin, R. G. Medhurst, "A Common Error in FM Distortion Theory," Proceedings of the IEEE, February, 1964.

48. E. J. Baghdady, "The FM Random-Noise Threshold," Frequency, March-April, 1963.

49. D. Middleton, "On Theoretical Signal-to-Noise Ratios in F-M Receivers: A Comparison with Amplitude Modulation," Journal of Applied Physics, April, 1949.

50. J. J. Downing, "Optimization and Evaluation of the Deviation-Compression [Frequency-Feedback] FM Demodulator," Lockheed Report, July, 1962.

APPENDIX I - NARROW BAND FM NOISE

The noise at the input to an FM receiver can generally be assumed to be "white," and thus a random stochastic process.

If this noise is passed through a narrow-band filter, it may be treated as a narrow-band random process. Such a process is described by the equation:

$$n(t) = V(t) \cos \left[\omega_c t + \phi (t) \right]$$

where $V(t)$ and $\phi(t)$ are random, slowly varying (as compared to $\omega_c t$) functions of time, the rate depending upon the bandwidth of the filter.

Expanding the above expression gives:

$$n(t) = V(t) \cos \omega_c t \cos \phi(t) - V(t) \sin \omega_c t \sin \phi(t).$$

Let:

$$y_c(t) = V(t) \cos \phi(t)$$

$$y_q(t) = V(t) \sin \phi(t).$$

Then:

$$n(t) = y_c(t) \cos \omega_c t - y_q(t) \sin \omega_c t .$$

Since y_c and y_q are random variables and can be considered to be sample functions, the central limit theorem guarantees that they are normally distributed.

Their independence can be proven by showing that their covariance, $\cos (y_c, y_q)$, is zero.

This is extensively covered by the literature; e.g., "Random Signals and Noise." [38]

The probability density function of y_c and y_q can now be expressed as:

$$p(y_c, y_q) = \frac{1}{2\pi\sigma^2} \exp\left\{ - \frac{1}{2\sigma^2} (y_c^2 + y_q^2) \right\}.$$

$P(V, \phi)$ can be obtained directly from $P(y_c, y_q)$ by transformation.

$$P(V, \phi) = \frac{1}{2\pi\sigma^2} \exp\left\{ - \frac{V^2}{2\sigma^2} \right\} \cdot \left| \begin{array}{cc} \frac{\partial V \cos\phi}{\partial V} & \frac{\partial V \sin\phi}{\partial V} \\ \frac{\partial V \cos\phi}{\partial \phi} & \frac{\partial V \sin\phi}{\partial \phi} \end{array} \right|$$

$$= \frac{1}{2\pi\sigma^2} \exp\left\{ - \frac{V^2}{2\partial^2} \right\}$$

where $V \geq 0$ and $0 \leq \phi \leq 2\pi$.

Integrating $P(V, \phi)$ with respect to V and ϕ gives:

$$P(\phi) = \frac{1}{2\pi}, \quad P(V) = \frac{V}{\sigma^2} \exp\left\{ - \frac{V^2}{2\sigma^2} \right\} \quad \text{respectively.}$$

Therefore:

$$P(V, \phi) = P(V)\, P(\phi).$$

V and ϕ are thus statistically independent random variables. Note also that V is Rayleigh distributed and ϕ is uniformly distributed from 0 to 2π.

APPENDIX II - DETECTION OF FM SIGNAL PLUS NOISE

Consider the IF signal input to the demodulator:

$$e_{IF} = e(t) + n(t)$$

$$= E \cos (\omega_{IF}t + \psi) + V \cos (\omega_{IF}t + \phi)$$

$$= E \cos (\omega_{IF}t + \psi) + V \cos (\omega_{IF}t + \psi) \cos (\psi - \phi)$$

$$+ V \sin (\omega_{IF}t + \psi) \sin (\psi - \phi).$$

Let:

$$X_c = V \cos (\psi - \phi)$$

$$X_q = V \sin (\psi - \phi).$$

Then:

$$e_{IF} = E \cos (\omega_{IF}t + \psi) + X_c \cos (\omega_{IF}t + \psi) + X_q \sin (\omega_{IF}t + \psi)$$

$$= \left[(E + X_c)^2 + X_q^2 \right]^{1/2} \cos \left[\omega_{IF}t + \psi - \tan \frac{X_q}{(E + X_c)} \right].$$

If this signal is now amplified and clipped to give a unity peak amplitude and then applied to a differentiator (or a frequency discriminator) with a unity slope factor, the resulting output will be:

$$e_d = - \left\{ \omega_{IF} + \dot{\psi} - \frac{d}{dt} \left[\tan^{-1} \left(\frac{X_q}{E + X_c} \right) \right] \right\} \sin \left[\omega_{IF}t + \psi - \tan^{-1} \left(\frac{X_q}{E + X_c} \right) \right]$$

If this signal is now applied to an amplitude detector, and a baseband filter, whose bandwidth is just wide enough to pass the baseband signal and eliminate the DC term (ω_{IF}), the demodulator output is obtained as:

$$e_o = \frac{d}{dt}\left[\tan^{-1}\left(\frac{X_q}{E + X_c}\right)\right] + \dot{\psi}$$

$$= \left[\frac{1}{1 + \left(\frac{X_q}{E + X_c}\right)^2}\right] \frac{d}{dt}\left(\frac{X_q}{E + X_c}\right) + \dot{\psi}$$

$$= \dot{\psi} + \frac{\dot{X}_q (E + X_c) - X_q \dot{X}_c}{(E + X_c)^2 + X_q^2}$$

$$= \dot{\psi} + \frac{\frac{\dot{X}_q}{E}\left(1 + \frac{X_c}{E}\right) - \frac{X_q \dot{X}_c}{E^2}}{\left(1 + \frac{X_c}{E}\right)^2 + \left(\frac{X_q}{E}\right)^2} .$$

APPENDIX III - MEAN SQUARE VALUE OF NOISE

Consider the noise signal:

$$n = \frac{\frac{\dot{X}_q}{E}\left(1 + \frac{\dot{X}_c}{E}\right) - \frac{\dot{X}_q \dot{X}_c}{E^2}}{\left(1 + \frac{X_c}{E}\right)^2 + \left(\frac{X_q}{E}\right)^2}$$

Let:

$$y_c = V \cos(\phi) = X_c \Big|_{\psi = 0}$$

$$y_q = V \sin(\phi) = -X_q \Big|_{\psi = 0}$$

where V and ϕ and statistically independent- Rayleigh and - uniformly (0-2π) distributed random variables, respectively.

According to S. O. Rice's paper, [8] the position of the threshold and the baseband signal-to-noise ratio above threshold region are affected very little by the presence of modulation. Above the threshold, a modulated signal, in fact, yields slightly less baseband noise than an unmodulated signal with the same IF signal-to-noise ratio. Therefore, y_c and y_q should be good approximations for X_c and X_q, respectively, above the threshold. Keep in mind that $y_c = X_c$ and $y_q = -X_q$ for an unmodulated carrier.

Thus:

$$\overline{n^2} = \overline{\left[\frac{\dot{y}_q \left(1 + \frac{y_c}{E}\right) - \frac{y_q \dot{y}_c}{E^2}}{\left(1 + \frac{y_c}{E}\right)^2 + \left(\frac{y_q}{E}\right)^2} \right]^2}$$

$$= \overline{\frac{\left(\frac{\dot{y}_q}{E} + \frac{y_c \dot{y}_q}{E^2} - \frac{y_q \dot{y}_c}{E^2}\right)^2}{\left(1 + \frac{2y_c}{E} + \frac{y_c^2}{E^2} + \frac{y_q^2}{E^2}\right)^2}} \quad .$$

Expanding the numerator and applying the binomial expansion to the denominator yields:

$$\overline{n^2} = \left[\frac{\dot{y}_q}{E^2} + \frac{2\dot{y}_q^2 y_c}{E^3} - \frac{2y_q' y_c' y_q}{E^3} + \frac{y_q'^2 y_c^2}{E^3} - \frac{2y_q' y_c' y_q y_c}{E^4} \right.$$

$$\left. + \frac{y_q^2 y_c'^2}{E^4} \right] \left[1 - \frac{4y_c}{E} - \frac{10y_c^2}{E^2} - \frac{2y_q^2}{E^2} - \frac{20y_c^3}{E^3} + \frac{12y_c y_q^2}{E^3} \right.$$

$$\left. - \frac{45y_c^4}{E^4} + \frac{3y_q^4}{E^4} - \frac{42y_c^2 y_q^2}{E^4} + \frac{80y_c^4}{E^4} + \cdots \right] .$$

The mean square value of a random function, in this case the noise, n, is the expectation of the square of the function.

$$\overline{n^2} = \int_{-\infty}^{+\infty} n^2 p(n)dn = \Sigma(n^2)$$

where P(n) is the probability density function of n.

As shown in Appendix I, the joint probability of V(t) and $\phi(t)$ is given by:

$$P(\, V(t),\, \phi(t)\,) = \frac{V(t)}{2\pi\sigma^2} \exp\left\{\frac{-\, V^2(t)}{2\sigma^2}\right\}$$

$$V(t) \geq 0 \qquad 0 \leq \phi(t) \leq 2\pi \,.$$

Then:

$$(y_c y_q) = \int_0^{\infty} \int_0^{2\pi} (y_c^{\,n}\, y_q^{\,m})\, p(V,\, \phi)\, d\phi\, dV$$

$$= \int_0^{\infty} \int_0^{2\pi} \frac{V(t)^{m+n+1} \cos^n(\,\phi(t)\,) \sin^m(\,\phi(t)\,)}{2\pi\sigma^2} \exp\left\{-\frac{V^2(t)}{2\sigma^2}\right\} d\phi(t)\, dV(t).$$

Applying this integral gives:

$$\overline{y_c} = \overline{y_q} = \overline{y_c^{\,3}} = \overline{y_q^{\,3}} = \overline{y_c y_q} \qquad \text{all other odd moments} = 0$$

$$\overline{y_c^2} = \overline{y_q^2} = \sigma^2$$

$$\overline{y_c^4} = \overline{y_q^4} = 3\sigma^4$$

$$\overline{y_c^2 y_q^2} = \sigma^4$$

etc.

In Appendix IV, it is shown that:

$$\overline{\dot{y}_q^2} = \overline{\dot{y}_c^2} .$$

Multiplying out the expression for $\overline{n^2}$ and substituting the above functions yields:

$$\overline{n^2} = \frac{\overline{\dot{y}_q^2}}{E^2} \left[1 + 2\frac{\sigma^2}{E^2} + \frac{8\sigma^4}{E^4} + \cdots \right].$$

APPENDIX IV - EVALUATION OF $\overline{\dot{X}_q^2}$

As in Appendix III, y_q will be used instead of X_q where:

$$y_q = - X_q \Big|_{\psi = 0} = V(t) \sin (\phi(t)) .$$

We may represent y_q by a Fourier Series:

$$y_q = \sum_{k=-\infty}^{\infty} (- a_k \sin 2\pi f_k t + b_k \cos 2\pi f_k t)$$

where a_k and b_k are independent, normally distributed variables with a zero mean and σ_k^2 variance.

Then:

$$\dot{y}_q = \sum_{k=-\infty}^{\infty} (2\pi f_k) (- a_k \cos 2\pi f_k t - b_k \sin 2\pi f_k t)$$

$$\overline{\dot{y}_q^2} = \overline{\sum_{k=-\infty} (2\pi f_k)^2 \left(a_k^2 \cos^2 2\pi f_k t + 2\, a_k b_k \cos 2\pi f_k t \sin 2\pi f_k t + b_k^2 \sin^2 2\pi f_k t\right)}$$

$$= \sum_{k=-\infty}^{\infty} (2\pi f_k)^2 \left(\sigma_k^2 \cos^2 2\pi f_k t + \sigma_k^2 \sin^2 2\pi f_k t\right)$$

$$= \sum_{k=-\infty}^{\infty} (2\pi f_k)^2 \sigma_k^2 .$$

The same procedure gives:

$$\overline{\dot{y}_c^2} = \sum_{k=-\infty}^{\infty} (2\pi f_k)^2 \sigma_k^2 .$$

Thus:

$$\overline{\dot{y}_c^2} = \overline{\dot{y}_q^2} .$$

Since the noise power can be assumed to be uniformly distributed across the IF bandwidth, BW_{IF}:

$$\sigma_k^2 = \frac{\sigma^2}{BW_{IF}}$$

where σ^2 is the variance of the noise.

Since the output noise is limited to the baseband bandwidth, BW_{bb}:

$$\overline{\dot{y}_q^2} = \int_{-BW_{bb}}^{BW_{bb}} (2\pi f)^2 \sigma_k^2 \, df = \int_{-BW_{bb}}^{BW_{bb}} \frac{4\pi^2 f^2 \sigma^2}{BW_{IF}} \, df = \frac{8\pi^2 (BW_{bb})^3 \sigma^2}{3(BW_{IF})} .$$

APPENDIX V

In an effort to determine the effect of the low pass filter in the FCFL upon the noise bandwidth at the oscillator output and at the detector input, the closed loop response was evaluated. This yielded the following equations (Eq. (32) and Eq. (33) in the text, respectively):

$$\left(\frac{\phi_{osc}}{\phi_{in}}\right)_{norm} = \frac{1 + A\beta}{\left[(1 + A\beta) - \frac{1}{k}\left(\frac{f}{f_b}\right)^2\right] + j\left(1 + \frac{1}{k}\right)\frac{f}{f_b}}$$

$$\left(\frac{\phi_{d}}{\phi_{in}}\right)_{norm} = \frac{(1 + A\beta)\left(1 + j\frac{f}{f_b}\right)}{\left[(1 + A\beta) - \frac{1}{k}\left(\frac{f}{f_b}\right)^2\right] + j\left(1 + \frac{1}{k}\right)\frac{f}{f_b}}$$

Using an IBM 1620 computer, the phase and magnitude curves for these two expressions were evaluated for several k's and Aβ's. These curves are shown in the following ten graphs.

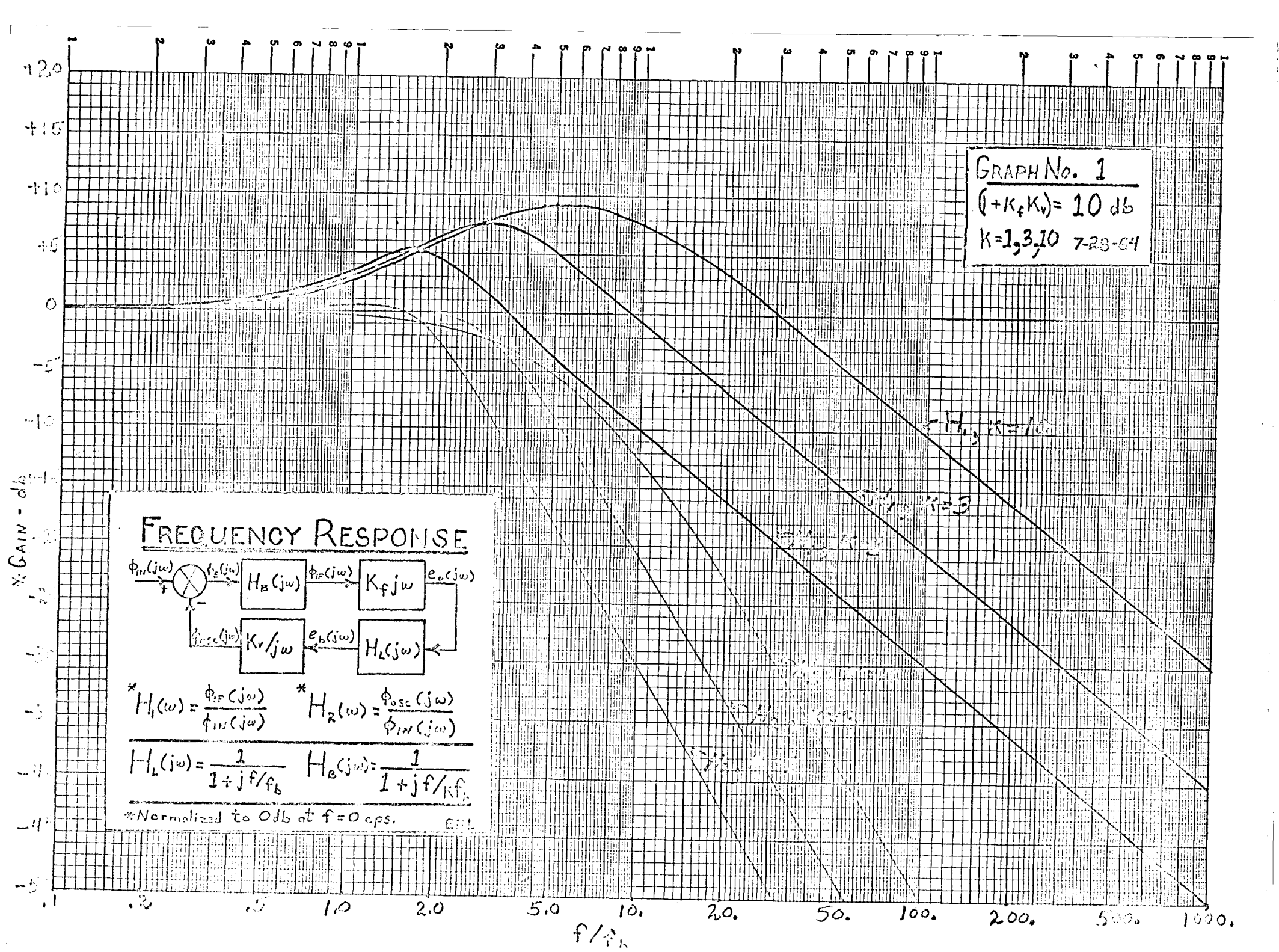
GRAPH No. 1
(1+K_f K_v) = 10 db
K = 1, 3, 10 7-28-64
FREQUENCY RESPONSE
φ_IN(jω)
φ_E(jω)
H_B(jω)
φ_IF(jω)
K_f jω
e_o(jω)
φ_OSC(jω)
K_v/jω
e_b(jω)
H_L(jω)
*H_1(ω) = φ_IF(jω) / φ_IN(jω)
*H_2(ω) = φ_OSC(jω) / φ_IN(jω)
H_L(jω) = 1 / (1 + jf/f_b)
H_B(jω) = 1 / (1 + jf/Kf_b)
*Normalized to 0db at f = 0 cps.
* GAIN - db
f/f_b
+20
+15
+10
+5
0
-5
-10
-15
-20
.1
.2
.5
1.0
2.0
5.0
10.
20.
50.
100.
200.
500.
1000.

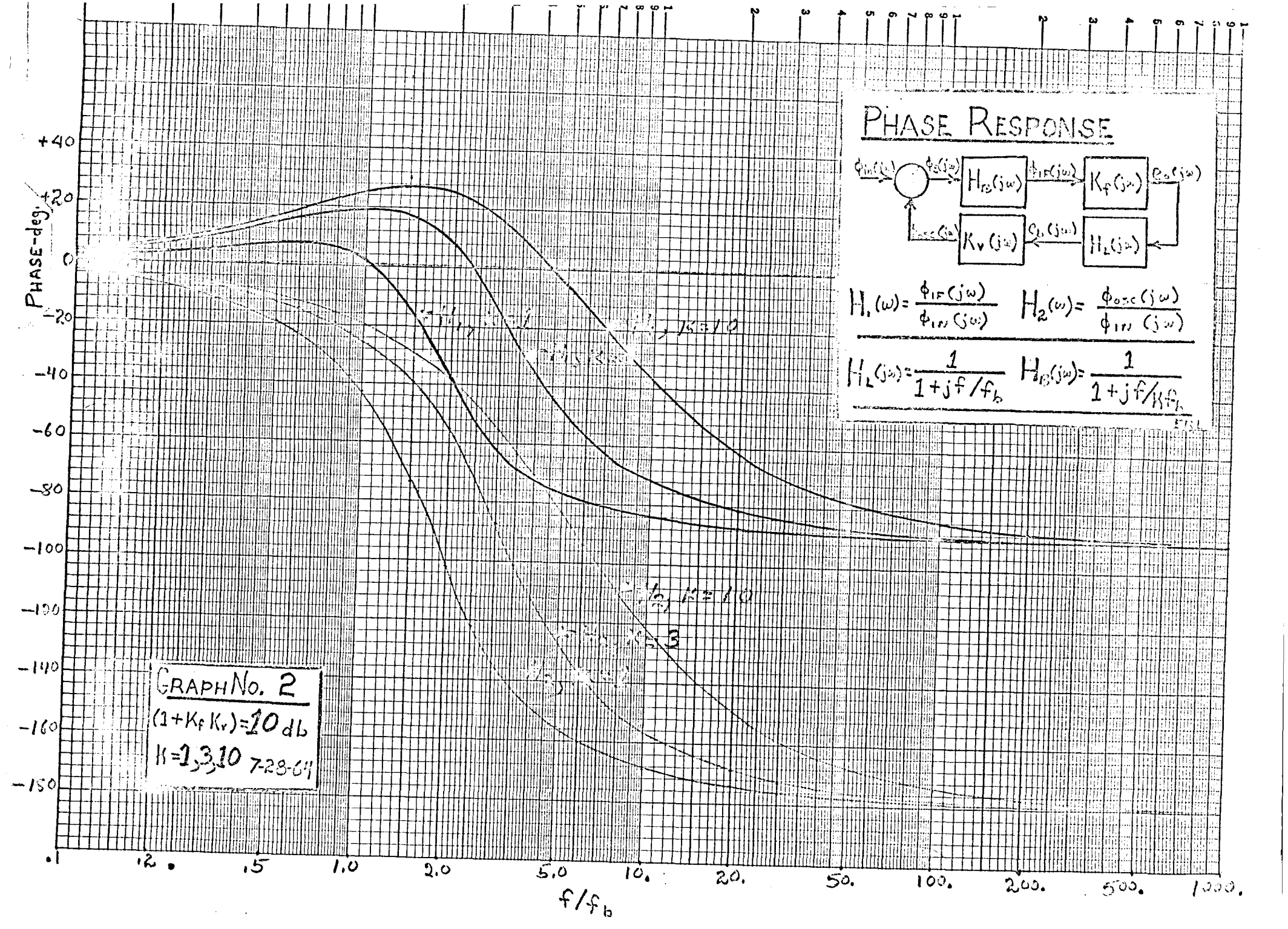
PHASE RESPONSE
$\phi_{in}(j\omega)$
$\phi_e(j\omega)$
$H_{fb}(j\omega)$
$\phi_{IF}(j\omega)$
$K_f(j\omega)$
$e_o(j\omega)$
$\phi_{osc}(j\omega)$
$K_v(j\omega)$
$e_b(j\omega)$
$H_L(j\omega)$
$H_1(\omega) = \frac{\phi_{IF}(j\omega)}{\phi_{in}(j\omega)}$
$H_2(\omega) = \frac{\phi_{osc}(j\omega)}{\phi_{in}(j\omega)}$
$H_L(j\omega) = \frac{1}{1+jf/f_b}$
$H_{fb}(j\omega) = \frac{1}{1+jf/K f_b}$
PHASE-deg.
+40
+20
0
-20
-40
-60
-80
-100
-120
-140
-160
-180
.1
.2
.5
1.0
2.0
5.0
10.
20.
50.
100.
200.
500.
1000.
f/f_b
$K = 10$
$K = 3$
GRAPH No. 2
$(1+K_f K_v) = 10$ db
K = 1, 3, 10 7-28-64

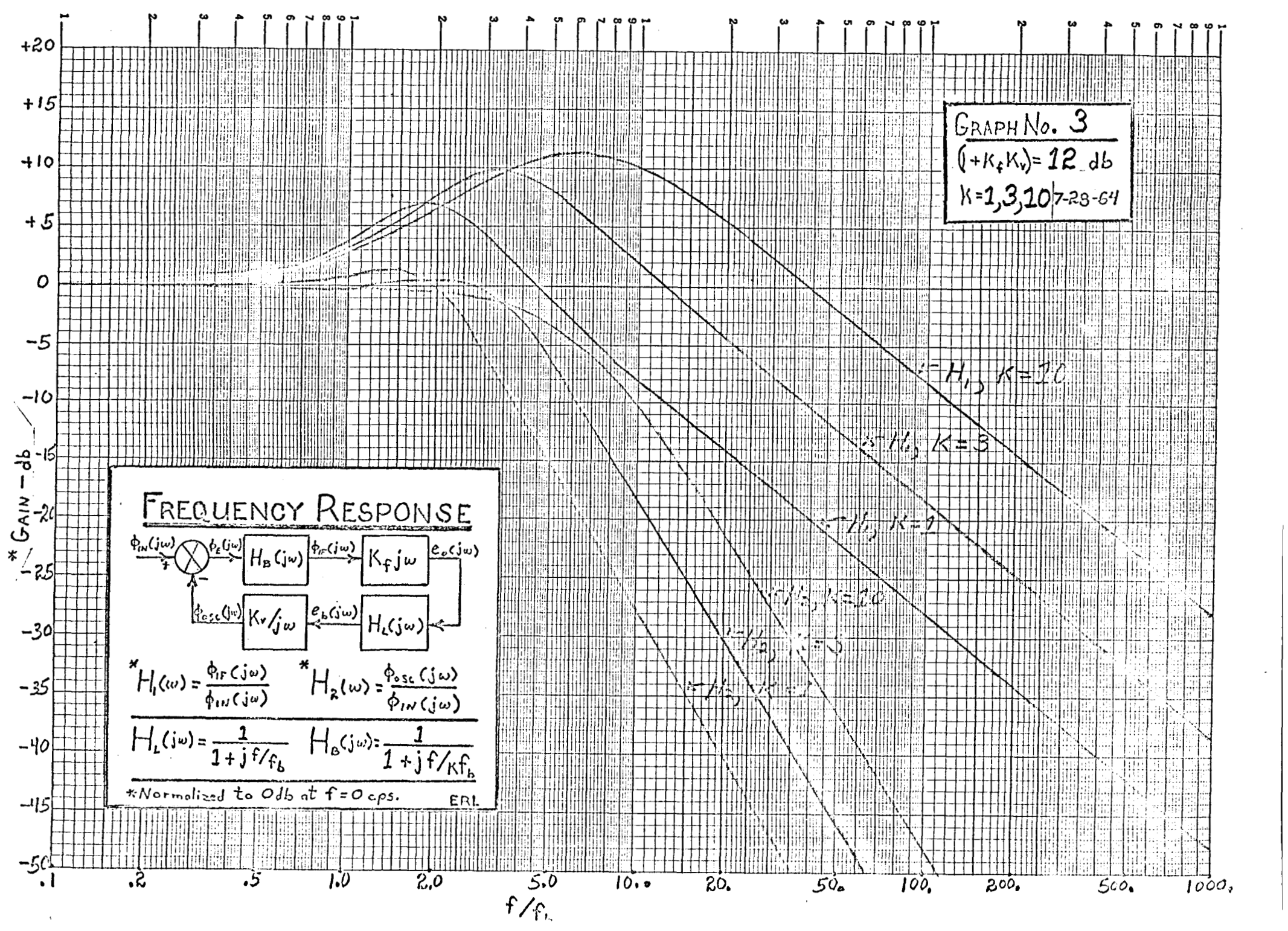
GRAPH No. 3
(1+K_f K_v) = 12 db
K = 1, 3, 10
7-28-64
FREQUENCY RESPONSE
φ_IN(jω)
φ_ε(jω)
H_B(jω)
φ_IF(jω)
K_f jω
e_o(jω)
φ_osc(jω)
K_v/jω
e_b(jω)
H_L(jω)
*H_1(ω) = φ_IF(jω) / φ_IN(jω)
*H_2(ω) = φ_osc(jω) / φ_IN(jω)
H_L(jω) = 1 / (1 + j f/f_b)
H_B(jω) = 1 / (1 + j f/Kf_b)
*Normalized to 0db at f = 0 cps.
ERL
* GAIN - db
f/f_b
+20
+15
+10
+5
0
-5
-10
-15
-20
-25
-30
-35
-40
-45
-50
.1
.2
.5
1.0
2.0
5.0
10.0
20.
50.
100.
200.
500.
1000.

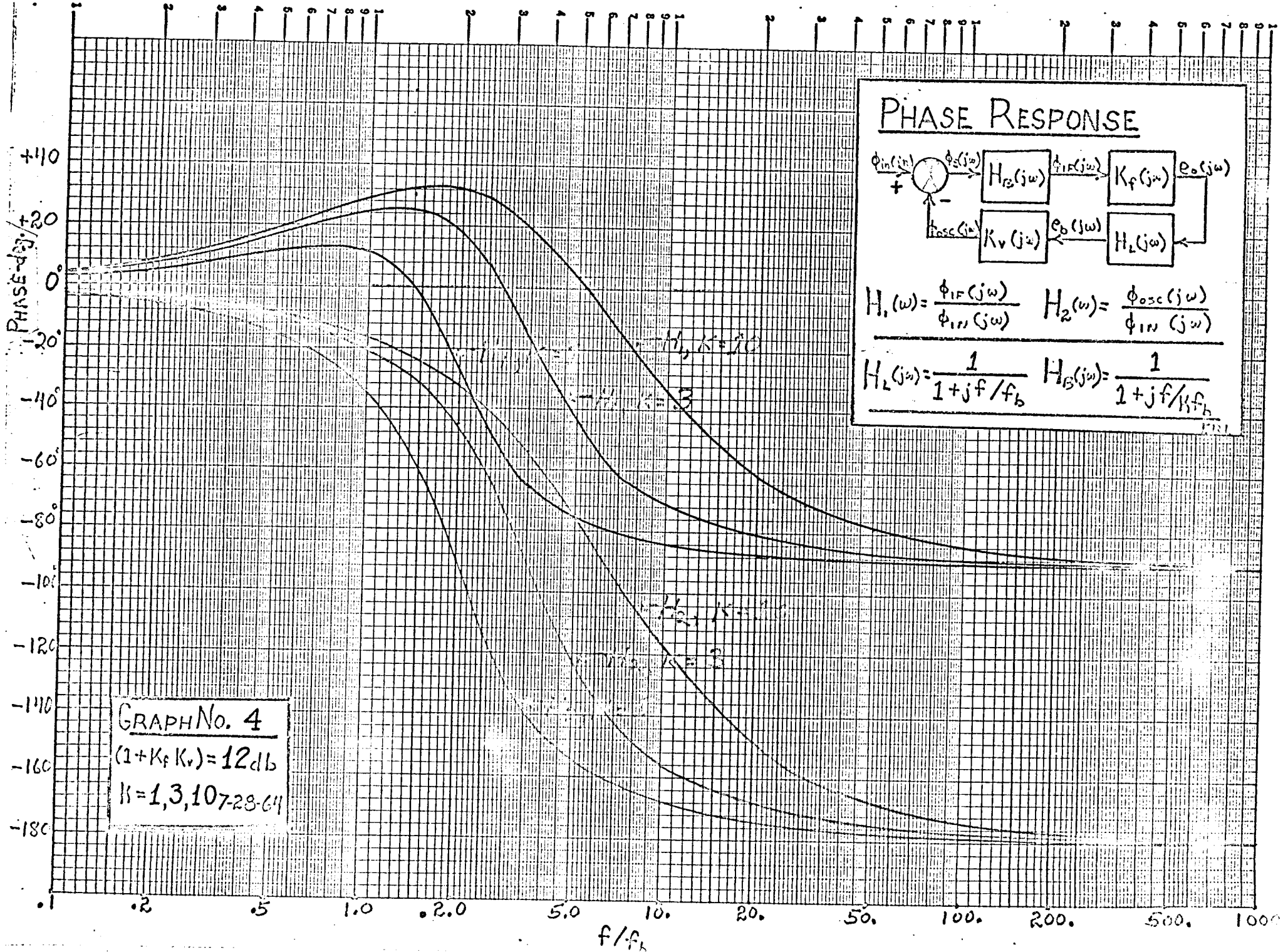
PHASE RESPONSE
$\phi_{in}(j\omega)$
$\phi_s(j\omega)$
$H_B(j\omega)$
$\phi_{IF}(j\omega)$
$K_f(j\omega)$
$e_o(j\omega)$
$\phi_{osc}(j\omega)$
$K_v(j\omega)$
$e_b(j\omega)$
$H_L(j\omega)$
$H_1(\omega) = \frac{\phi_{IF}(j\omega)}{\phi_{in}(j\omega)}$ $H_2(\omega) = \frac{\phi_{osc}(j\omega)}{\phi_{in}(j\omega)}$
$H_L(j\omega) = \frac{1}{1+jf/f_b}$ $H_B(j\omega) = \frac{1}{1+jf/Kf_b}$
PHASE-deg./+20
+40
0°
-20°
-40°
-60°
-80°
-100
-120
-140
-160
-180
.1
.2
.5
1.0
2.0
5.0
10.
20.
50.
100.
200.
500.
1000
f/f_b
GRAPH No. 4
(1+K_f K_v) = 12 db
K = 1, 3, 10 7-28-64

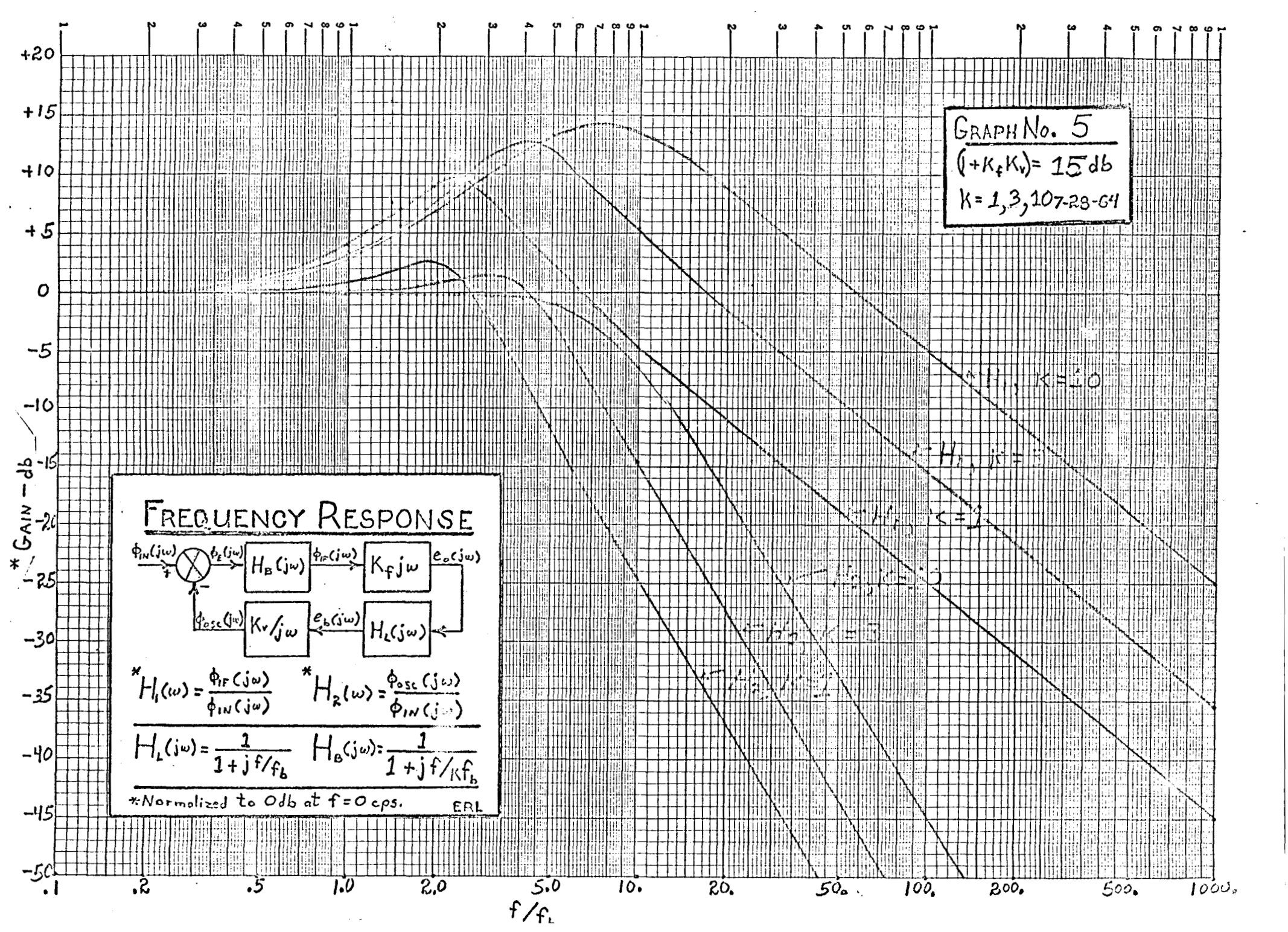
GRAPH No. 5
$(1+K_f K_v)$ = 15 db
K = 1,3,10
7-28-64
FREQUENCY RESPONSE
$\phi_{IN}(j\omega)$
$\phi_E(j\omega)$
$H_B(j\omega)$
$\phi_{IF}(j\omega)$
$K_f j\omega$
$e_o(j\omega)$
$\phi_{osc}(j\omega)$
$K_v/j\omega$
$e_b(j\omega)$
$H_L(j\omega)$
$*H_1(\omega) = \frac{\phi_{IF}(j\omega)}{\phi_{IN}(j\omega)}$
$*H_2(\omega) = \frac{\phi_{osc}(j\omega)}{\phi_{IN}(j\omega)}$
$H_L(j\omega) = \frac{1}{1+jf/f_b}$
$H_B(j\omega) = \frac{1}{1+jf/Kf_b}$
*Normalized to 0db at f = 0 cps.
ERL
* GAIN - db
+20
+15
+10
+5
0
-5
-10
-15
-20
-25
-30
-35
-40
-45
-50
.1
.2
.5
1.0
2.0
5.0
10.
20.
50.
100.
200.
500.
1000.
f/f_L

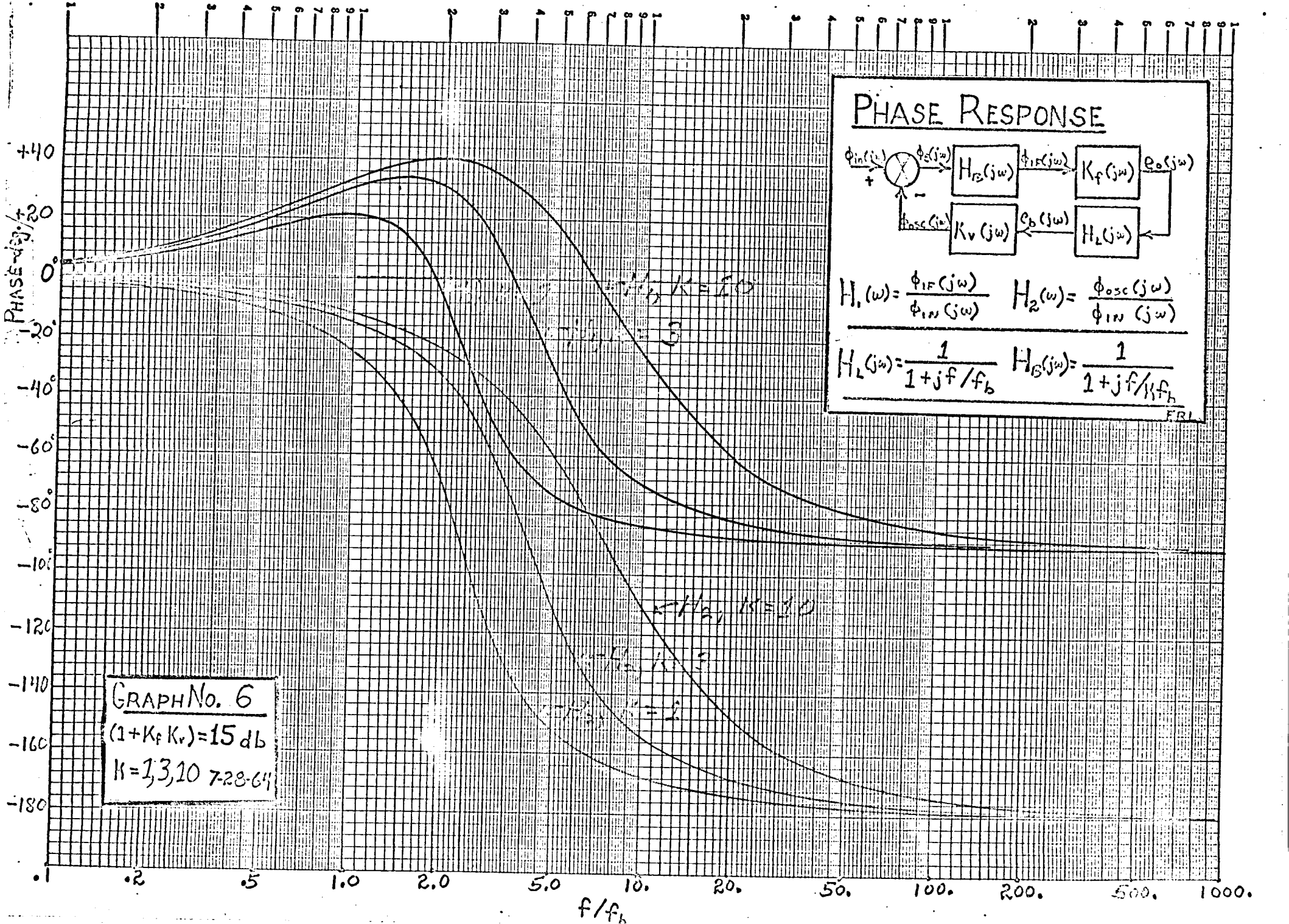
PHASE RESPONSE
$\phi_{in}(j\omega)$
$\phi_E(j\omega)$
$H_E(j\omega)$
$\phi_{IF}(j\omega)$
$K_f(j\omega)$
$e_o(j\omega)$
$\phi_{osc}(j\omega)$
$K_v(j\omega)$
$e_b(j\omega)$
$H_L(j\omega)$
$H_1(\omega) = \frac{\phi_{IF}(j\omega)}{\phi_{IN}(j\omega)}$ $H_2(\omega) = \frac{\phi_{osc}(j\omega)}{\phi_{IN}(j\omega)}$
$H_L(j\omega) = \frac{1}{1+jf/f_b}$ $H_E(j\omega) = \frac{1}{1+jf/Kf_b}$
FBL
GRAPH No. 6
$(1+K_f K_v) = 15$ db
K = 1, 3, 10 7-28-64
PHASE
+40
+20
0°
-20°
-40°
-60°
-80°
-100°
-120
-140
-160
-180
.1
.2
.5
1.0
2.0
5.0
10.
20.
50.
100.
200.
500.
1000.
f/f_b

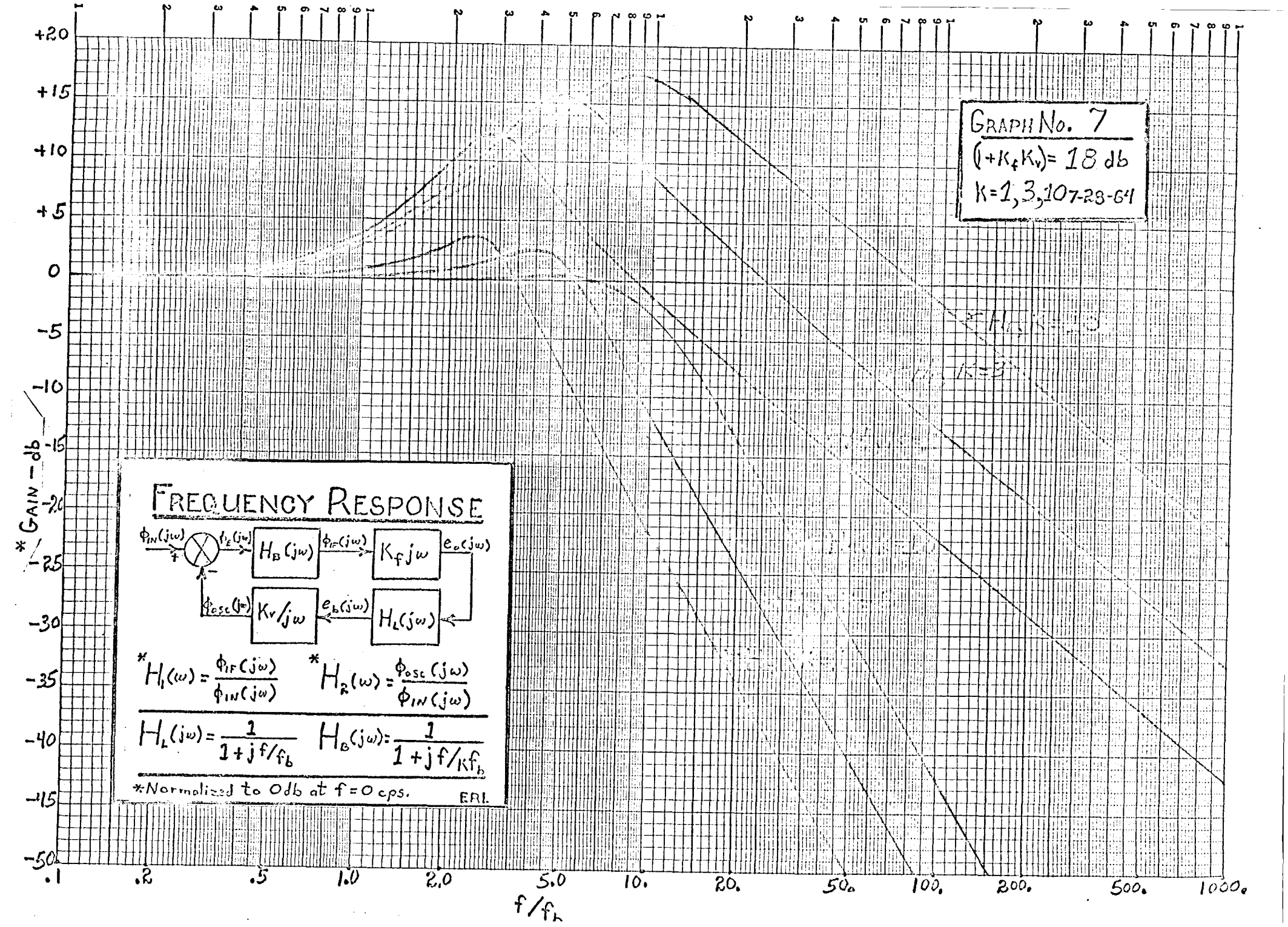
GRAPH No. 7
$(1+K_f K_v)$ = 18 db
K = 1, 3, 10 7-23-64
K=10
K=3
K=1
FREQUENCY RESPONSE
$\phi_{IN}(j\omega)$
$H_B(j\omega)$
$\phi_{IF}(j\omega)$
$K_f j\omega$
$e_o(j\omega)$
$\phi_{osc}(j\omega)$
$K_v/j\omega$
$e_b(j\omega)$
$H_L(j\omega)$
$^*H_1(\omega) = \frac{\phi_{IF}(j\omega)}{\phi_{IN}(j\omega)}$
$^*H_2(\omega) = \frac{\phi_{osc}(j\omega)}{\phi_{IN}(j\omega)}$
$H_L(j\omega) = \frac{1}{1+jf/f_b}$
$H_B(j\omega) = \frac{1}{1+jf/Kf_b}$
*Normalized to 0db at f = 0 cps.
ERI.
* GAIN - db
+20
+15
+10
+5
0
-5
-10
-15
-20
-25
-30
-35
-40
-45
-50
.1
.2
.5
1.0
2.0
5.0
10.
20.
50.
100.
200.
500.
1000.
f/f_b

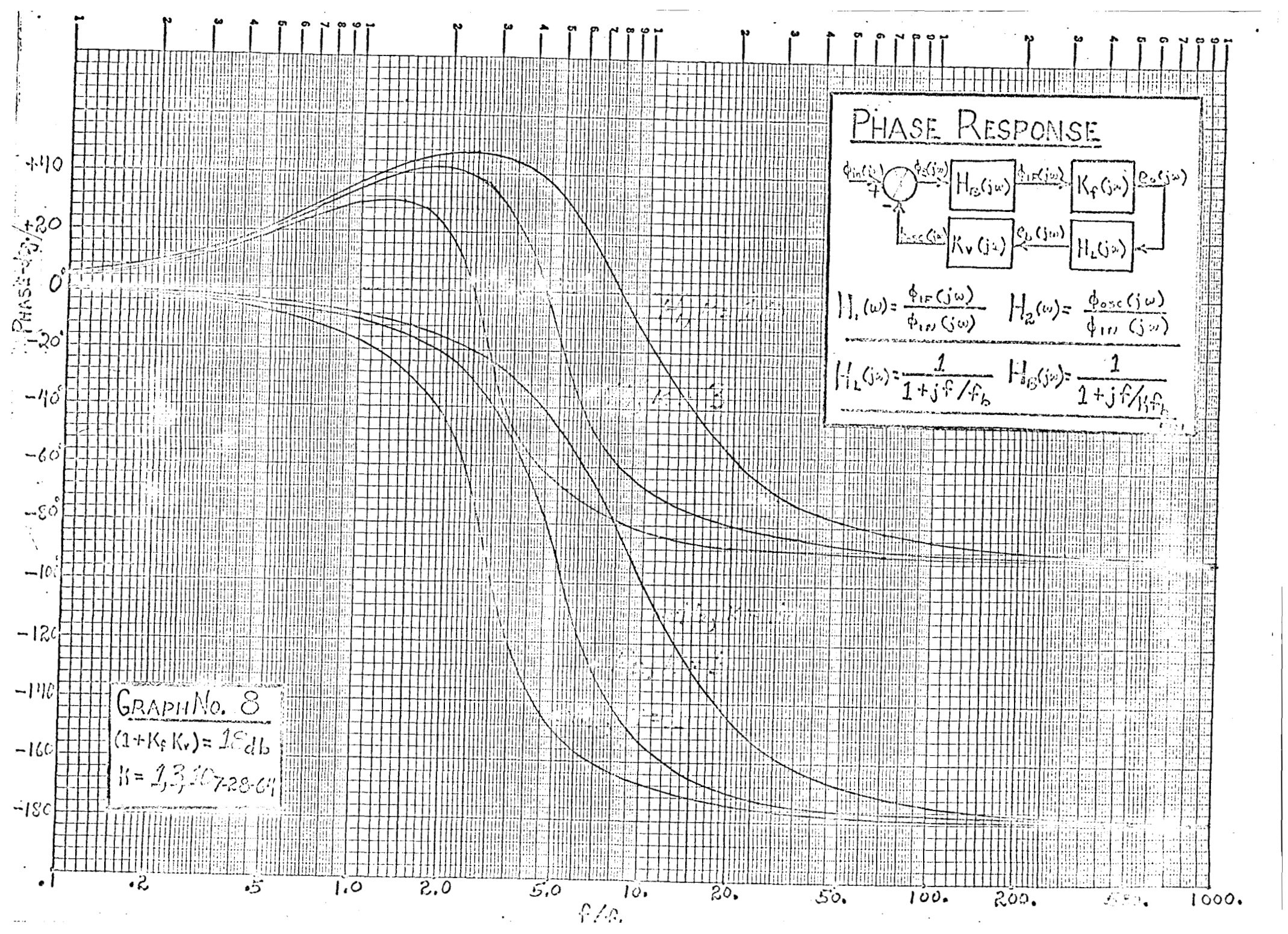
PHASE RESPONSE
$\phi_{in}(j\omega)$
$\phi_e(j\omega)$
$H_{1B}(j\omega)$
$\phi_{IF}(j\omega)$
$K_f(j\omega)$
$e_o(j\omega)$
$\phi_{osc}(j\omega)$
$K_v(j\omega)$
$e_b(j\omega)$
$H_L(j\omega)$
$H_1(\omega) = \frac{\phi_{IF}(j\omega)}{\phi_{in}(j\omega)}$ $H_2(\omega) = \frac{\phi_{osc}(j\omega)}{\phi_{in}(j\omega)}$
$H_L(j\omega) = \frac{1}{1+jf/f_b}$ $H_{1B}(j\omega) = \frac{1}{1+jf/K_1 f_b}$
GRAPH No. 8
$(1+K_f K_v) = 18$ db
K = 1,310 7-28-64
+40
+20
0°
-20°
-40°
-60°
-80°
-100
-120
-140
-160
-180
PHASE-φ(jω)
.1
.2
.5
1.0
2.0
5.0
10.
20.
50.
100.
200.
500.
1000.
f/fb

GRAPH No. 9

$(1+K_f K_v) = 20$ db

$K = 1, 3, 10$ 7-23-51

FREQUENCY RESPONSE

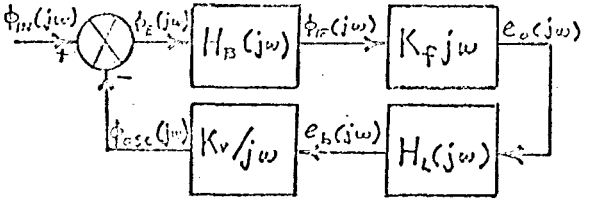

$$*H_1(\omega) = \frac{\phi_{IF}(j\omega)}{\phi_{IN}(j\omega)} \qquad *H_2(\omega) = \frac{\phi_{osc}(j\omega)}{\phi_{IN}(j\omega)}$$

$$H_L(j\omega) = \frac{1}{1 + jf/f_b} \qquad H_B(j\omega) = \frac{1}{1 + jf/Kf_b}$$

*Normalized to 0db at f = 0 cps. FBL

* GAIN — db

+20, +15, +10, +5, 0, -5, -10, -15, -20, -25, -30, -35, -40, -45, -50

.1, .2, .5, 1.0, 2.0, 5.0, 10., 20., 50., 100., 200., 500., 1000.

f/c

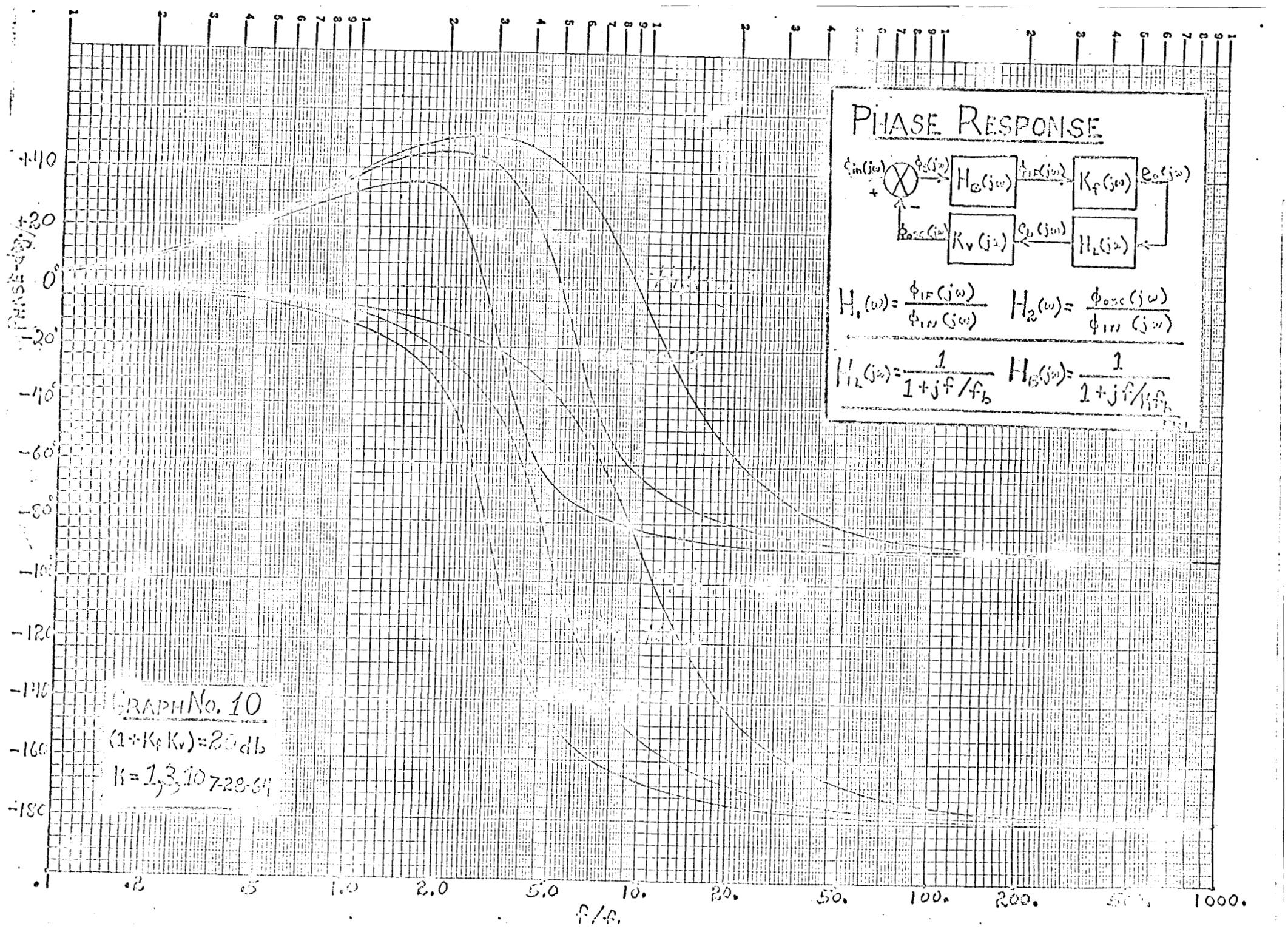
PHASE RESPONSE
$\phi_{in}(j\omega)$
$\phi_e(j\omega)$
$H_e(j\omega)$
$\phi_{IF}(j\omega)$
$K_f(j\omega)$
$e_o(j\omega)$
$\phi_{osc}(j\omega)$
$K_v(j\omega)$
$e_b(j\omega)$
$H_L(j\omega)$
$H_1(\omega) = \frac{\phi_{IF}(j\omega)}{\phi_{IN}(j\omega)}$
$H_2(\omega) = \frac{\phi_{osc}(j\omega)}{\phi_{IN}(j\omega)}$
$H_L(j\omega) = \frac{1}{1+jf/f_b}$
$H_e(j\omega) = \frac{1}{1+jf/K_f f_b}$
PHASE $-\phi_2$ °/+20
+40
0°
-20°
-40°
-60°
-80°
-100
-120
-140
-160
-180
.1
.2
.5
1.0
2.0
5.0
10.
20.
50.
100.
200.
1000.
f/f$_b$
GRAPH No. 10
$(1+K_f K_v)$ = 20 db
K = 1, 3, 10 7-29-64